Third-day road log, from Alpine, Arizona, to Luna, Reserve, Apache Creek, Horse Springs and Datil, New Mexico

James C. Ratte, D. J. Bove, S. M. Cather, R. M. Chamberlin, S. G. Crews, and W. C. McIntosh
1994, pp. 79-111. https://doi.org/10.56577/FFC-45.79

in:

Mogollon Slope (West-Central New Mexico and East-Central Arizona), Chamberlin, R. M.; Kues, B. S.; Cather, S. M.; Barker, J. M.; McIntosh, W. C.; [eds.], New Mexico Geological Society 45th Annual Fall Field Conference Guidebook, 335 p. https://doi.org/10.56577/FFC-45

This page is intentionally left blank to maintain order of facing pages.

THIRD-DAY ROAD LOG, FROM ALPINE, ARIZONA, TO LUNA, RESERVE, APACHE CREEK, HORSE SPRINGS AND DATIL, NEW MEXICO

J. C. RATTÉ, D. J. BOVE, S. M. CATHER, R. M. CHAMBERLIN, S. G. CREWS and W. C. MCINTOSH

SATURDAY, OCTOBER 1, 1994

Assembly Point: Alpine Country Club
Departure Time: 7:00 a.m. MST (Arizona Time)
8:00 a.m. MDT (New Mexico Time)
Distance: 130.7 mi
Stops: 4

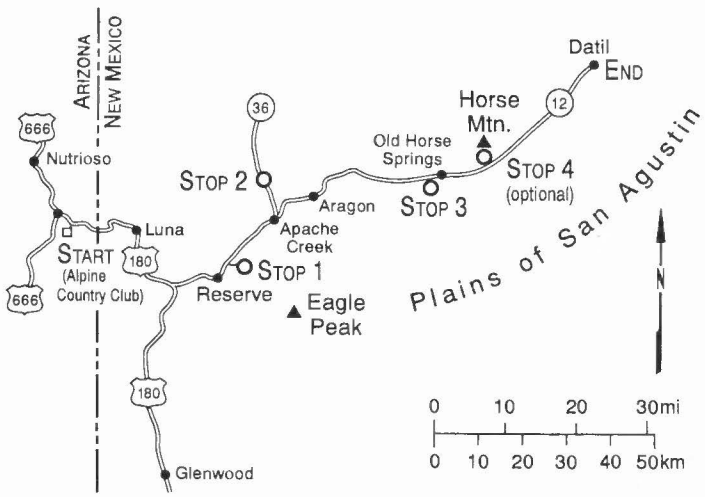

SUMMARY

On Day 3, the trip departs from the Alpine, Arizona Country Club, where we will have assembled for breakfast, starting at 6:00 a.m. Arizona Time! (7:00 a.m., NM time). Starting at Alpine, in the footwall of the Reserve graben system, the Third-Day route follows US-180 east, via Luna, New Mexico, descending into the Reserve graben across several tilted, half-graben blocks. Between Luna, and the junction of US-180 and NM-12, we pass through the recent landslide areas in Mail Hollow and Dry Leggett Canyon, which disrupted traffic for several weeks in Fall 1992. At the junction of US-180 and NM-12, we turn north and follow NM-12 through Reserve and north to the Eagle Peak road, where we turn east. Stop 1 is in the deepest part of the Reserve graben, along the Tularosa River north of Reserve, where we will discuss the evolution of the graben structure, sedimentology of the Gila Formation (Oligocene to Pliocene), and the local volcanic stratigraphy. Stop 1A, nearby, provides an opportunity to see a basalt flow interlayered in the Gila Formation and to examine a small reverse fault that is related to a small- scale buttress unconformity.

Upon returning to NM-12, we continue north to Apache Creek, where we take NM-32 northwest for about 9 mi to Stop 2, where relatively new roadcuts expose volcaniclastic sediments of the Spears Group (Eocene and Oligocene) beneath andesite lava flows of Dry Leggett Canyon (~34 Ma). Here we discuss the provenance and sedimentary structures in this sequence of well-sorted sandstones, the origin of numerous, thin, pink ash-beds interlayered with the sandstones, and the origin of the black fiamme and the pink, bedded deposits in which they occur, between andesite flows.

After we return to Apache Creek, we continue east on NM-12 to Old Horse Springs, Stop 3. At this stop, we examine pyroclastic deposits at the eruptive center of the Horse Springs dacite (informal unit), and *mineralized* jasperoid inclusions (silicified pre-Tertiary limestone, quartzite and argillaceous rocks), with skarn-type reaction rims. From this vantage point, we can also discuss the structure of the San Agustin half graben as revealed by seismic profiles, the small hogback of pre-Tertiary rocks (Laramide high?) at the foot of the Horse Mountain volcano on the northern margin of the graben, the alignment of Bearwallow Mountain volcanoes on its southern margin, and the results of the recent oil play in this region.

Stop 4 is at the small hogback of Permian sedimentary rocks at the base of Horse Mountain on the north side of NM-12, about 6 mi east of Old Horse Springs. This is an optional stop, and there may not be sufficient time on this field trip to examine these outcrops that are believed to represent the Mogollon Rim, a relict of the Laramide uplift at the southeast margin of the Colorado Plateau in this area. Tertiary stratigraphic nomenclature used in this third-day road log follows the proposals of Cather et al. (this volume).

Mileage

0.0	Alpine Country Club Dining Room and Clubhouse parking lot. Return to US-180.	**0.2**
0.2	**Keep left**, past "SLOW" sign.	**0.7**
0.9	**Turn left** onto road from Blue River and proceed to US-180.	**0.9**
1.8	Junction with US-180; **turn right**.	**0.2**
2.0	MP (Milepost) 430. Luna Lake north of highway, on	

left. Entrance to Luna Lake Recreation Site and Campground about 0.25 mi ahead on left.

Intermediate to mafic composition lava flows and volcaniclastic sedimentary rocks exposed along the highway between here and the Luna quadrangle have not been mapped in detail, and little is known of the local structural geology. The closest detailed mapping is in the Alpine-Nutrioso area to the north (Wrucke, 1961), the Blue Range Primitive area to the south (Ratté et al., 1969), and the Luna quadrangle to the east (T.L. Finnell, unpubl. geologic map, 1985). Based on these studies and roadside reconnaissance, we know that the volcanic sequence in this area is essentially the same as that in adjacent parts of New Mexico. Bloodgood Canyon Tuff (Oligocene) from the Bursum caldera in the Mogollon Mountains, about 30 mi to the southeast, is present both north and south of Alpine, and provides a structural benchmark for our descent into the Reserve graben system to the east.

In terms of the new stratigraphic terminology proposed for the volcanic and volcaniclastic rocks of the Mogollon-Datil volcanic field (Cather et al., this volume), the sedimentary rocks exposed along US-180 between here and the Luna quadrangle are all within the Eocene-Oligocene Spears Group, and the intermediate to mafic lava flows are probably all andesite of Dry Leggett Canyon (~ 34 Ma) in the upper part of the Eocene-Oligocene Datil Group. **0.6**

2.6 Luna Lake Dam on left; brown sandstone above andesite of Dry Leggett Canyon(?) flows exposed in spillway. **0.4**

3.0 MP 431. Andesite flows across valley north of highway. Brown sandstone in roadcuts on south side of highway. From the highway at about MP 431, views of Turner Peak, to northeast (left), on the New Mexico-Arizona border, about 4 mi away. Light-colored rocks forming Matterhorn-like edifice on south side of Turner Peak (Figs. 3.1, 3.2) is a volcanic neck that probably fed the andesitic lava flows that cap Turner Peak. The andesitic flows, of uncertain age, overlie volcaniclastic rocks in the upper part of the Spears Group, above the andesite of Dry Leggett Canyon. In addition, the neck includes a vent-breccia margin that contains blocks, up to several meters long, of silicic ash-flow tuff (Davis Canyon(?) Tuff), and is cut by thin, irregular rhyolite dikes that contain sanidine and biotite. **2.0**

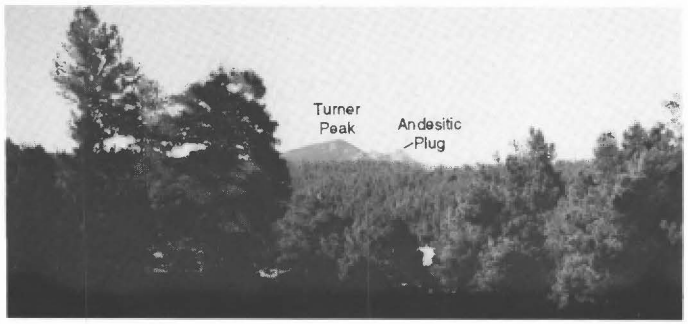

FIGURE 3.1 View of Turner Peak and andesitic eruptive center along Arizona-New Mexico state line from US-180 at about Mile Post (MP) 431. Turner Peak and eruptive center are about 4 mi away.

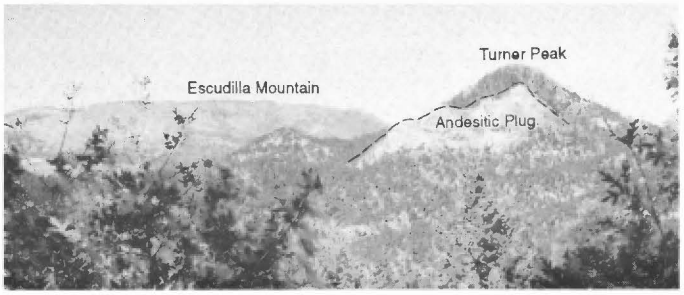

FIGURE 3.2. View of Turner Peak and eruptive center from point about 1.8 mi southeast of the peak.

5.0 MP 433. Arizona-New Mexico state line just ahead. **0.3**

5.3 Arizona-New Mexico state line. **0.5**

5.8 Porphyritic lava flows along both sides of the highway are correlated with andesite of Dry Leggett Canyon; they have phenocrysts of plagioclase and both clinopyroxene and orthopyroxene. **1.1**

6.9 Base of andesite flows of Dry Leggett Canyon overlying brown mudflow breccias in lower part of Spears Group. Watch for 3-7 ft of interlayered ash-flow tuff in roadcuts on left just ahead, between here and MP 2. Pink, densely welded tuff is overlain by light-gray, punky, partly welded tuff; both are probably tuff of Bishop Peak (34.7 Ma) which was mapped near here by T.L. Finnell (unpubl., 1982). **0.4**

7.3 MP 2. More outcrops, or slumped blocks, of ignimbrite just west of MP-2. Highway crosses approximately located, northwest-trending normal fault in the next 0.25 mi. On the east side of the fault, the andesite of Dry Leggett Canyon and the overlying sandstones are downdropped about 425 ft. **1.2**

8.5 San Francisco River. Andesite of Dry Leggett Canyon on both sides of river. East of bridge, road follows approximately along contact between andesite and overlying brown sandstone. A few miles north of the road are small, anomalous exposures of Pennsylvanian strata, discussed in the following minipaper. **0.8**

FAUNA FROM A SMALL PENNSYLVANIAN EXPOSURE NEAR LUNA, NEW MEXICO

Barry S. Kues

**Department of Earth & Planetary Sciences,
University of New Mexico, Albuquerque, NM 87131-1116**

Two small exposures of Pennsylvanian strata occur within the Tertiary volcanic terrane near Luna. First reported by Foster (1957), they were mapped by Weber and Willard (1959), and the largest (Trout Creek) outcrop was described by Kottlowski (1959, 1960). This outcrop is about 7 mi northwest of Luna, along Forest Road 220, about 5.3 mi north of its intersection with F.R. 219, in the NE¼ NW¼ sec. 10, T5N, R21W, Catron County. The section, as measured by Kottlowski (1960, p. 26-27, fig. 5) consists primarily of steeply-dipping beds of gray or pink calcarenite and limestone, totaling 350-400 ft thick, which contain crinoid columnals, unbroken brachiopods, fusulinids (*Fusulina*, now *Beedeina*), corals and algae. The fusulinids suggested a probable Desmoinesian (Middle Pennsylvanian) age. This small exposure shows

no evidence of baking or intrusion by the surrounding Tertiary igneous rocks, and is either a float block in the volcanic terrane or a small, upthrown fault block (Kottlowski, 1960). Similar small, isolated exposures of Virgilian or Wolfcampian limestones, assigned questionably to the Naco Formation, occur about 7 mi to the west, just inside Arizona, and were interpreted as probable inclusions in andesites of the Datil Formation (Wrucke, 1961). I visited the larger Luna exposure in 1988 to collect macrofossils that might verify the suggested Desmoinesian age, and here report briefly on the nature of the invertebrate fauna. These fossils were collected mainly from Kottlowski's unit 8, near the top of the section, a pinkish, coarsely crystalline, bioclastic limestone unit containing chert nodules locally. Preservation of the fossils is generally poor, owing to weathering and difficulty in extracting complete specimens from the hard limestone matrix.

The fauna consists chiefly of brachiopods, bryozoans, and crinoid stem segments. Among bryozoans, compact, massive to encrusting, fistuliporoid zoaria are most abundant; *Fenestella* and ?*Rhombopora* are much less common. Brachiopods are represented by at least eight species. The unornamented, biconvex athyrid *Composita subtilita* (Hall) is the most abundant brachiopod. Specimens are up to about 32 mm long, and display a wide variability in shape, as is typical of this species (Figs. 3.3A-C). Specimens range from relatively narrow to slightly wider than long, and possess a conspicuous fold and sulcus on the brachial and pedicle valves.

A second athyrid species, *Cleiothyridina pecosii* (Marcou), is smaller and has less convex valves than *C. subtilita*. The valves are slightly to moderately wider than long; a typical specimen is 13.5 mm wide and 11.5 mm long. The valves display many conspicuous growth lamellae, each with numerous, simple, small, narrow, closely-spaced spines extending posteriorly along the valve surface to or past the next lamella. On most specimens only short, somewhat flattened spine bases are preserved, and even these are obscure on worn specimens (Fig. 3.3E). However, one specimen (Fig. 3.3D) displays numerous complete spines, some more than 2 mm long. Dunbar and Condra (1932) noted of *C. orbicularis* (now known to be a synonym of *C. pecosii*; see Sutherland and Harlow, 1973), that the spines "when preserved from a mat that hides the body of the shell," which would apply equally well to unworn examples from the Luna outcrop.

Neospirifer alatus Dunbar and Condra (Figs. 3.3G-H) is common in all growth stages. Specimens attain a maximum width of more than 70 mm (twice the length), and are characterized by up to 15 ribs within the sulcus, 25 to 30 plications on the lateral slopes, of which those nearest the sulcus display early trifurcation, and by conspicuous fasciculation of the lateral plications. Smaller, relatively alate spiriferids with 10-13 bold, rounded, uniformly simple lateral plications, three to (more commonly) five plicae within the sulcus, and four (less commonly six) plicae on the fold are assigned to *Anthracospirifer* aff. *A. curvilateralis chavezae* Sutherland and Harlow (Fig. 3.3F). The largest specimen measures about 25 mm wide and 21 mm long. These specimens appear to fall within the range of variation documented for the subspecies by Sutherland and Harlow (1973), but no complete specimens are available that would allow definite identification.

A single small spiriferid pedicle valve (Fig. 3.3I), about 8 mm wide by 5.5 mm long, displays a rather high cardinal area and eight strong, broadly rounded plications, of which the central two are largest and most widely spaced. This specimen is quite similar to, although smaller than, New Mexico Morrowan specimens of *Spiriferellina campestris* (White) (see especially Sutherland and Harlow, 1973, pl. 18, fig. 1b). The surface of the valve is weathered and partially exfoliated, and does not display the tiny pustules typical of the genus. Its strong plications and absence of a well-defined sulcus immediately distinguish this specimen from juveniles of *N. alatus* and *A.* aff *A. curvilateralis chavezae*.

Productoid brachiopods are moderately common, but very incomplete and too poorly preserved to allow positive identification. *Linoproductus* sp. (Figs. 3.3J-K) attains an estimated length of about 45 mm, lacks a median sinus on the umbo, possesses relatively fine costallae (8-10/5 mm about 20 mm surface length from the beak), and virtually lacks spine bases. Specimens referred to *Antiquatonia* cf. *A. hermosana* (Girty) (Fig. 3.3L) have relatively sharp radial costae crossed by concentric wrinkles, producing elongate nodes at the intersection points on the anterior surface of the pedicle valve. The number of radial costae is about 10-12/10 mm at a distance of about 25-30 mm from the beak, within the range for Desmoinesian specimens of *A. hermosana* (Sutherland and Harlow, 1973). Shape, convexity, and hingeline features could not be accurately determined from the specimens at hand, however. A medium-sized (width to 35+ mm) species of

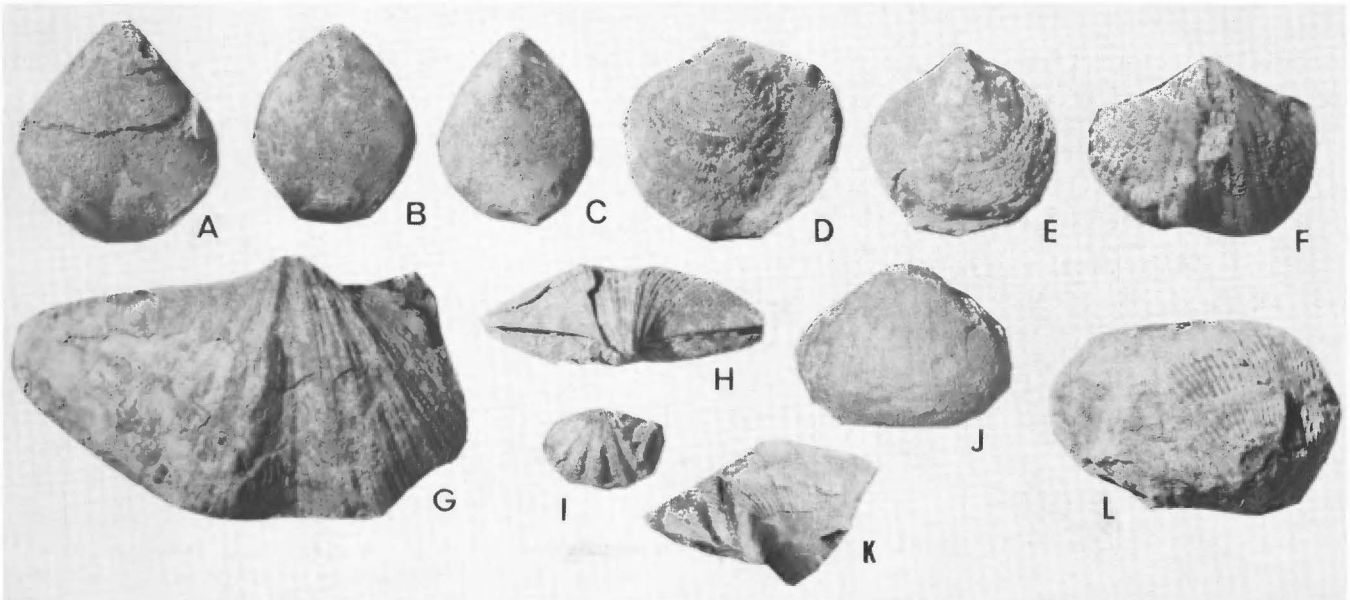

FIGURE 3.3. Pennsylvanian brachiopods from north of Luna, New Mexico; all figures natural size unless otherwise indicated. A-C, *Composita subtilita*, pedicle valve, UNM 11,972; and pedicle and brachial valves, UNM 11,973. D-E, *Cleiothyridina pecosii*, pedicle valve showing well preserved fine spines, UNM 11,974, and somewhat worn brachial valve, UNM 11,975. F, *Anthracospirifer* aff. *A. curvilateralis chavezae*, pedicle valve, UNM 11,976, x 1.5. G-H, *Neospirifer alatus*, pedicle valve of a large specimen, UNM 11,977; and hinge view, UNM 11,978. I, *Spiriferellina* cf. *S. campestris*, pedicle valve, UNM 11,979, x2. J-K, *Linoproductus* sp., pedicle valve, UNM 11,980; and oblique posterior view of a fragmentary pedicle valve, UNM 11,981. L, *Antiquatonia* cf. *A. hermosana*, oblique posterior view of incomplete pedicle valve, UNM 11,982.

Derbyia, possibly *D. haesitans*, is common in this fauna. The valves are significantly wider than long, and bear sharp, high, fairly widely spaced radial costellae with smaller ones in the interspaces. The brachial valve is moderately convex and the pedicle valve nearly flat. As none of the specimens is complete, specific identification was not attempted.

Two incomplete bivalve steinkerns, one a myalinid, the other unidentifiable, were also collected at this locality.

Most of the identifiable brachiopods are relatively long-ranging taxa, that together are consistent with a Desmoinesian or Missourian age. The younger age is slightly favored by the presence of *Neospirifer alatus*, which is known only from the Missourian in New Mexico (Sutherland and Harlow, 1973) and ranges from the Missourian to Virgilian in Kansas (Spencer, 1967).

I thank Frank E. Kottlowski for providing some information relating to this locality.

9.3 MP 4. Brown sandstone on north side of highway. Andesite of Dry Leggett Canyon is faulted up above highway on an approximately east-west fault that is tangent to the highway curve just ahead. **0.6**

9.9 Approximate western edge of the Luna 7-1/2' quadrangle (Finnell, unpubl., 1985). Outcrops along highway are mainly andesite flows of Dry Leggett Canyon. **0.4**

10.3 MP 5. Andesitic flows on both sides of highway; downhill, ahead, volcaniclastic sedimentary rocks have sub-horizontal dips that change to 10-15° westward approaching the Luna fault. **1.0**

11.3 MP 6. Highway descends back into valley of San Francisco River. Sharp curve to left, ahead; highway now along Luna fault, within the northeast-trending Blue-Luna-Spur Lake fault zone (Fig. 3.4). **0.9**

12.2 Cattleguard. Western margin of the Luna half graben, where the Luna fault controls the northwest edge of Luna Valley, site of the historic town of Luna, directly ahead. Volcaniclastic rocks in the lower part of the Spears Group and Gila Formation conglomerate are juxtaposed across the fault. Gila Formation crops out left of cattleguard about 300 ft ahead. **0.6**

12.8 Road junction in the town of Luna; **stay on US-180**, which curves sharply right to bridge across San Francisco River. **0.4**

HISTORICAL VIGNETTE OF THE TOWN OF LUNA, CATRON COUNTY, NEW MEXICO

J.C. Ratté

U.S. Geological Survey, P.O. Box 25046, MS 905, Denver, CO 80225

The Luna Valley was first settled by Mormon families from southern Utah in 1883 (Luna Ward-The Church of Jesus Christ of Latter-day Saints, 1983), although the brothers Luna had been grazing sheep in the valley for more than 10 years prior. The settlers voted to call their town "Grant," but Grants, New Mexico had precedence, and the Post Office Department finally accepted Luna, named for Don Solomon Luna, who was the leader of the Republican party in New Mexico

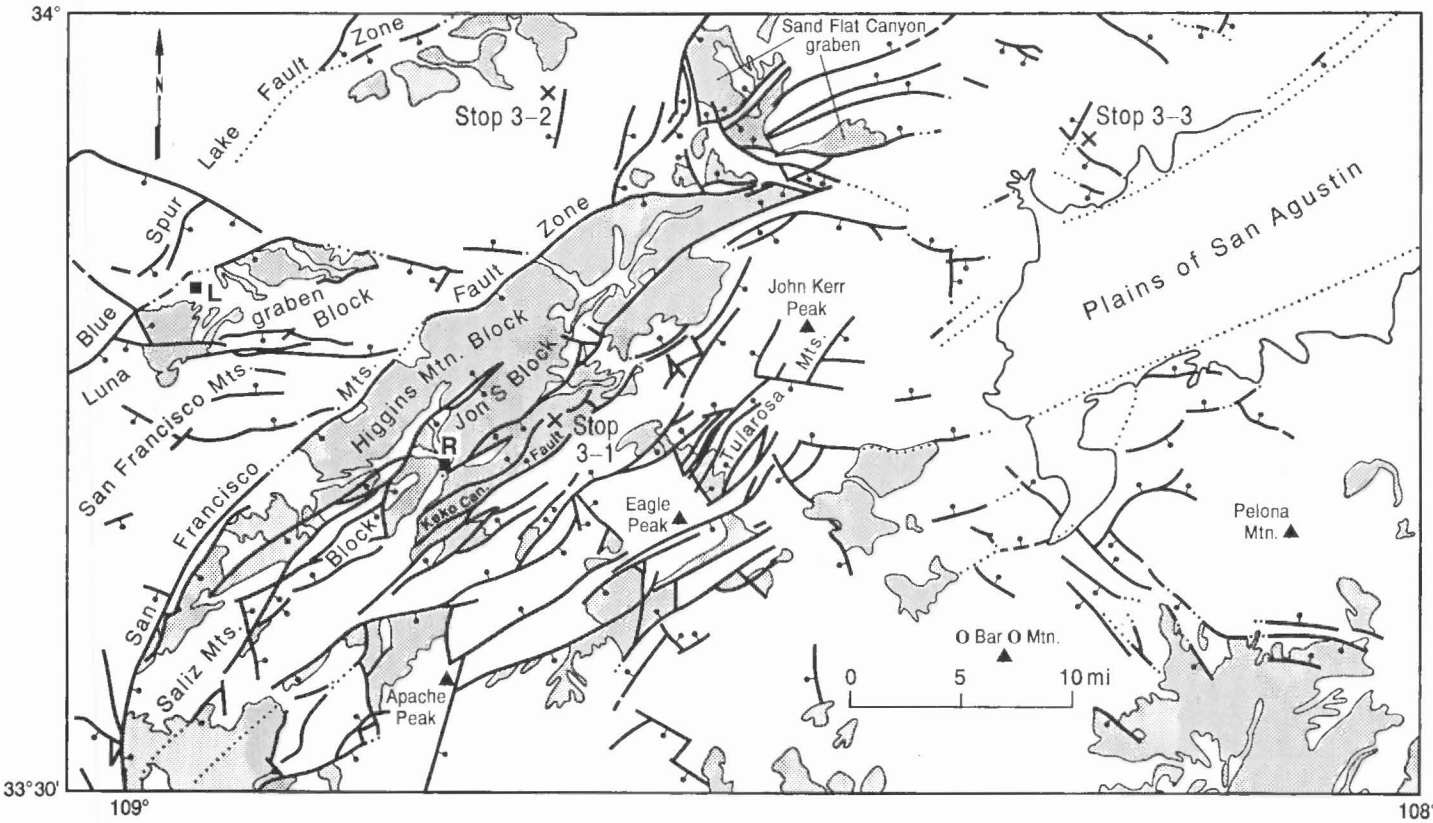

FIGURE 3.4. Generalized geologic map of the Reserve graben system between Luna and the Tularosa Mountains east of Reserve, New Mexico, showing major tilted fault blocks, and distribution of Gila Formation volcaniclastic rocks (shaded) **L**, Luna; **R**, Reserve.

Territory and in the State for more than 25 years (Pearce, 1965). There is a somewhat indirect geological connection here in that Estella and Luna Leopold, who both were once members of the U.S. Geological Survey, are descendants of the Luna and Leopold families. This is an interesting union between the New Mexico sheep ranchers who gave their name to the town of Luna, and the Leopold family of Wisconsin, which is perhaps best known through Aldo Leopold, one of the earliest conservation advocates, author of "A Sand County Almanac" (Leopold, 1966), and "father" of the first Wilderness Area, the Gila, established by the U.S. Forest Service in the Gila National Forest in southwestern New Mexico in 1924. Estella, a professor in the Department of Botany at the University of Washington in Seattle, was formerly a palynologist with the Branch of Paleontology and Stratigraphy, USGS in Denver. Estella's brother, Luna, now on the faculty of the University of California at Berkeley, was formerly Chief Hydrologist of the U.S. Geological Survey.

We thank Eloisa Brown of Albuquerque, New Mexico, cousin of Estella Leopold, for verifying the family history included here.

13.2 MP 8. Near south end of bridge across San Francisco River. View down Luna Valley to east, left, where San Francisco River disappears from view in box canyon on the southeast side of the Luna graben. Low ridge across valley about 2 mi east of bridge is basalt flow, ~2.5 Ma (Marvin et al., 1989, p. 49), which is representative of numerous young basalt flows and cinder cones in this area on the southeast margins of the Colorado Plateau. The Luna basalt flow follows a relict drainage alignment that crossed the Luna graben prior to the establishment of the present San Francisco River in this area.

From bridge, US-180 continues south across alluvium and low ridges of Gila Formation graben-fill, which laps onto the northwest-tilted San Francisco Mountains block of the Reserve graben. Dips in the Gila Formation here in the Luna Valley are generally about 5-6° northward. **3.0**

16.2 MP 11. Leaving Gila Formation basin-fill deposits at eastern margin of Luna half graben. Highway starts ascent of Mail Hollow to the top of the San Francisco Mountains tilted fault block. Outcrops along the road from here to divide between Mail Hollow and Dry Leggett Canyon consist mainly of distal outflow of rhyolitic ash-flow tuffs from the caldera-related eruptive centers in the Mogollon Mountains, about 25 mi to the southeast, and interlayered volcaniclastic sedimentary rocks in the Spears Group. The San Francisco Mountains block is intricately broken by minor east-west-trending normal faults (Fig. 3.4) in the Luna and Dillon Mountain quadrangles. **0.5**

16.7 Light-gray, nearly white, Davis Canyon Tuff (29 Ma) in slopes along left side of highway is overlain by Shelly Peak and Bloodgood Canyon Tuffs (28 Ma) and interlayered volcaniclastic rocks. Tuffs are 16-50 ft thick. Davis Canyon Tuff is underlain by crossbedded dune sands and lenticular torrential conglomerate beds (Fig. 3.5) that emphasize the desert setting in this area in late Oligocene time. **1.1**

17.8 Southern border of Luna quadrangle; enter Bull Basin quadrangle (Ratté, 1989). **0.4**

18.2 MP 13. Approximate center of highway slide-repair area (see Gallagher, this volume). **1.0**

19.2 MP 14. Road to Saddle Mountain Lookout Tower on right. **0.1**

FIGURE 3-5. Crossbedded dune sands and torrential conglomerate lenses in Spears Group in Mail Hollow, Luna Quadrangle.

19.3 Mail Hollow divide; Potato Patch road on left. Begin descent of Dry Leggett Canyon to the San Francisco Mountains fault zone at the foot of the canyon. Outcrops in roadcuts for the next 1.5 mi are part of the alluvial facies of the Pueblo Creek Formation (Ratté, 1989), now redefined as part of the lower Spears Group. These rocks grade into the proximal andesitic vent facies (now included with the upper part of the Datil Group), which dominates the formation farther southwest, where central vent andesitic volcanoes erupted prior to deposition of the Davis Canyon Tuff. **0.5**

19.8 Heifer Basin overlook on left, at new highway scenic rest stop, with views across Heifer Basin to Tularosa Mountains on the east side of the Reserve graben (Fig. 3.6). Rocks in Heifer Basin and along highway ahead are brown, mudflow breccias of the lower part of the Spears Group, overlain at the head of the basin by the ash-flow tuff sequence of the Miocene and Oligocene

FIGURE 3.6. Heifer Basin overlook; view northeast to Tularosa Mountains on the east side of the Reserve graben, on skyline at far right. Thin, discontinuous tuff lenses, **t**, are interlayered with mudflow breccia layers in upper part of Spears Group, which is overlain by ash-flow tuffs of the Mogollon Group, capping the ridge at the head of the basin.

Mogollon Group (Davis Canyon, Shelley Peak and Bloodgood Canyon tuffs). Other thin, white, discontinuous tuffs are interlayered in the upper part of the mudflow sequence and can be seen from the overlook. Hells Mesa Tuff (32 Ma), from the Socorro cauldron, may be one of the thin tuffs in this section, but efforts to date and correlate these discontinuous and sometimes reworked tuffs with regional tuffs in the upper part of the Datil Group have been largely unsuccessful. Although some of these unidentified tuffs have quartz and sanidine phenocrysts like Hells Mesa Tuff, the only dated samples, in the Luna quadrangle, have Ar/Ar ages of 33.29 ± 0.14 Ma and 33.62 ± 0.1 Ma, in the age range of the Box Canyon Tuff, derived from uncertain source(s) in the southern part of the Mogollon-Datil field (McIntosh et al., 1991; 1992, p. 864). Two outcrops of the thin tuffs are exposed on the left side of the road just ahead. **0.3**

20.1 MP 15; cattleguard and road on left. One of the thin tuffs is exposed beside the highway just beyond the cattleguard. A small fault offsets this 8-in.-thick tuff about 7 ft. **0.6**

20.7 Cattleguard on right. Contact between mudflows in Spears Group and underlying andesitic lava flows of Dry Leggett Canyon. About 250 ft up road from contact, another thin tuff (less than 3 ft thick) may be exposed, if not obscured by recent road work.

The pyroxene-plagioclase andesite flows in Dry Leggett Canyon are about 1000 ft thick beneath Prairie Point Peak, north of the highway. Flow boundaries are irregular and obscure. These andesite flows are widespread in the northwest part of the 1:100,000-scale Tularosa Mountains quadrangle and adjacent parts of the Quemado 1:100,000 quadrangle. Sources for these flows are unknown in the Bull Basin quadrangle or elsewhere, except for one probable dike in the slopes above the highway, below Prairie Point Peak, and a possible domal eruptive center in the Saliz Pass quadrangle (Ratté, 1969) to the south. The andesite is highly altered locally to yellowish-brown clay, carbonate and silica by fumarolic activity; the flows may have been erupted onto water-saturated ground or into standing water. "Luna blue" agate, much sought by rockhounds, is found largely within and near the base of these andesite flows, and probably formed as a result of the fumarolic activity. Irregular altered zones are well exposed in fresh roadcuts in the canyon, but distinct flow boundaries are less common. **1.4**

22.1 MP 17. Site of overrun of blasted material produced during widening of highway (see Gallagher, this volume). **0.3**

22.4 Around sharp curve to left, basal contact of andesitic lava flows above lower part of volcaniclastic sequence of Spears Group. Clasts in these sedimentary rocks are commonly red and well rounded in contrast to clasts in the gray to brown mudflows that characterize much of the sequence above the Dry Leggett Canyon flows. Some of the sedimentary beds beneath the Dry Leggett Canyon flows contain clasts of pre-Tertiary rocks (Precambrian granite, quartzite and fossiliferous Paleozoic limestone) as well as Tertiary volcanic rocks. Thus the lower part of the Spears Group here is probably transitional to the Eocene Baca Formation, and where the conglomerate contains less than 50% volcanic clasts it should be mapped as Baca. However, no Baca Formation was mapped in the Bull Basin quadrangle (Ratté, 1989) because of the limited area of Baca-type outcrops, and the uncertain location of the gradational contact. **0.4**

22.8 Entering paleolandslide area (Fig. 3.7). This old landslide on the north side of Dry Leggett Canyon is the location of two of the highway repair projects (Gallagher's 18.54 and 18.66) described in the article by Gallagher (this volume). Clean-up work and new highway construction here has largely eliminated the evidence of the recent mobilization of this slide area. The problem of landslides and highways in New Mexico is discussed in the following minipaper. **0.5**

LANDSLIDES AND HIGHWAY MAINTENANCE IN NEW MEXICO

Susan Gallagher

New Mexico Department of Highways and Transportation, Santa Fe, NM 87504

Every year New Mexico experiences landslides throughout mountainous areas of the State. They usually occur in the spring when the winter snows melt, or in the summer once the summer rains begin. The addition of water can increase soil moisture pore pressure to create an unstable soil condition and cause a landslide or mudflow. Evidence of this appears as a jagged scarp face at the top of the slide area and a noticeable hummock of soil above the toe of the slide. Leaning trees are an obvious indicator of an active or potential slide area.

Typically, special crews of the New Mexico State Highway Department repair smaller slide areas, while larger ones are contracted out, depending on the type and amount of equipment needed. The slide repair designs are done in-house by the Geo-technical Section of the New Mexico State Highway Department.

Designing a landslide correction is an involved process. It includes site investigation, inclinometer installation, soil sampling, and field and laboratory testing. Factors considered in design include unit weight of soil, cohesion, phi angle, depth to slip surface, and depth to water table. Various computerized slope stability programs are used to determine stability. The landslide, at the time of failure, is assumed to have a safety factor equal to or less than 0.9. A slide correction is designed for a minimum safety factor of 1.25. This means that the forces resisting a failure are at least 25% greater than the driving forces, i.e. those attempting to create another slide. Once a 1.25 safety factor is achieved, the most economical design is selected.

Over the past five years, New Mexico has spent an average of $1,250,000 per year on slide repairs. This usually takes care of one or two large remediations that are contracted out, and materials for two or three small ones that are repaired with our own special crews.

The types of landslides that we have to deal with most frequently in New Mexico include rotational, translational and mudflows. The slides generally occur in either roadway fills or cutslopes. Inclinometers are routinely installed at slide areas to monitor the movement. Where a high water content is present, piezometers are installed to monitor water levels. Remedies vary from installing horizontal drains and french drains for dewatering a slope, to building a berm at the toe to stabilize the mass, to excavating the failed material and replacing it with a select fill, which may be layered with reinforcing geogrid. Corrective action has not always produced the desired result, in which

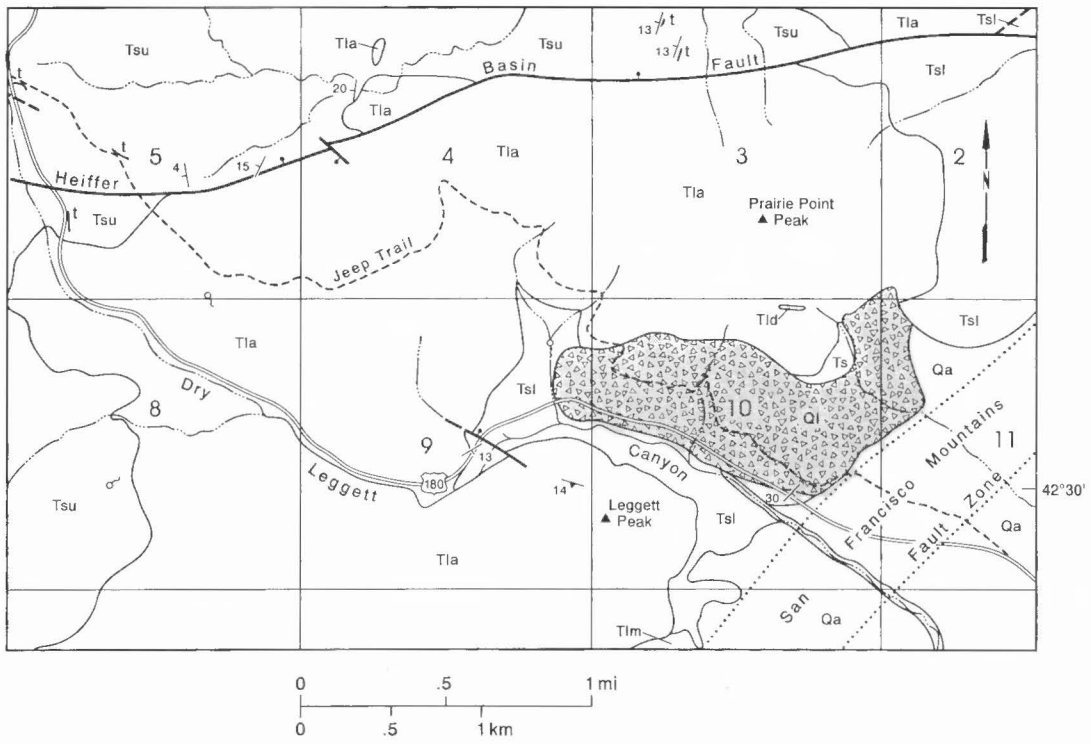

FIGURE 3.7. Geologic map showing the Prairie Peak paleolandslide on the north side of Dry Leggett Canyon and US-180. Landslide was remobilized during highway repairs in Fall 1992. **Qa**, Quaternary alluvium; **Ql**, Quaternary paleolandslide debris (patterned); **Tlm**, porphyritic quartz diorite intrusion (~ 15 Ma) south of Leggett Peak; **Tsu**, upper Spears Group and **Tsl**, lower Spears group volcaniclastic sedimentary rocks; **Tla**, andesite of Dry Leggett Canyon; **t**, discontinuous tuffs interlayered in upper Datil Group. Adapted from Ratté (1989).

case more monitoring is performed and the slide is reevaluated. In most cases the slide is stabilized. Although landslide remediation in highway construction is still more of an art than a science, improved instrumentation for data collection and computer-aided design have increased our capability for coping with this perennial problem.

23.3 Note drain pipes in slide area. **0.4**

23.7 Roadcut on north (left) side of highway in rounded boulder conglomerate containing abundant pre-Tertiary clasts, as well as Tertiary volcanic clasts (Fig. 3.8). Moderate to steep dips are probably related to deformation along the San Francisco Mountains fault zone, which bounds the footwall of the San Francisco Mountains tilted block, just ahead. The conglomerate in this roadcut represents a small exposure of the Baca Formation in the Bull Basin quadrangle. Prominent topographic nose, or buttress, about 0.6 mi south of highway at mountain front, east of Leggett Peak (Fig. 3.7) is a small intrusion of Miocene quartz diorite (~ 16 Ma), one of several silicic volcanic or sub-volcanic intrusive and eruptive centers within the Reserve graben; the intrusion here is along the San Francisco Mountains fault zone. **0.2**

23.9 Highway crosses trace of west strand of San Francisco Mountains fault zone. **0.8**

24.7 East border of Bull Basin quadrangle; enter Reserve 7½' quadrangle. MP 20 just ahead. **0.9**

25.6 Highway junction, US-180 and NM-12; **turn left on NM-12. Continue north** on alluvium-mantled surface. **0.6**

26.2 Entrance to Reserve airport on right. Good exposures of Gila Formation in roadcuts ahead. **1.3**

27.5 Cross bridge; dip slope of Brushy-Saliz Mountains tilted block to east (right). San Francisco Mountains fault zone at base of range-front scarp to west. **1.1**

28.6 MP 3. Cross S U Canyon. Gila Formation along highway fills half graben east of San Francisco Mountains fault zone and laps onto westward-dipping Brushy-Saliz Mountains tilted block east of highway. Brushy-Saliz Mountains block bifurcates into Higgins

FIGURE 3.8. East-dipping beds of conglomerate in Baca Formation at lower end of Dry Leggett Canyon on the north side of US-180, adjacent to the San Francisco Mountains fault zone near the east edge of the Bull Basin quadrangle.

Mountain and Jon S Mountain blocks of Crews (1990) north of Starkweather Canyon, just ahead. **1.5**

30.1 Cross Starkweather Canyon. Roadcuts in Gila Formation, on left, dip about 13°, somewhat less than the 15-20° dips of the underlying volcanic rocks, ahead in Starkweather Canyon. This change in attitudes is interpreted to be the result of differential tilt of the sedimentary rocks that were deposited during rotation of the Brushy-Saliz Mountains block, but an alternative explanation could be an additional fault that displaces Gila beds at the base of the dip slope east of the highway. North of Starkweather Canyon, the complex Brushy-Saliz Mountains tilted block was divided into the Higgins Mountain and Jon S-Enid sub-blocks by Crews (1990, p. 123-181), who used the Reserve graben as a field model for his doctoral dissertation at the University of Wyoming. **0.4**

30.5 Higgins Ranch road on left. Roadcuts ahead, from here to the highway bridge at the lower end of Starkweather Canyon, provide a stratigraphic descent through a 100-ft-thick sequence of typical, thin (16-33 ft) aa flows of Bearwallow Mountain Andesite (Oligocene and Miocene). Beneath the Bearwallow Mountain Andesite, Bloodgood Canyon Tuff varies from nearly white, cavernous weathering, poorly welded tuff to eutaxitic, densely welded tuff. The Bloodgood Canyon Tuff is separated from the underlying, red Shelley Peak Tuff (exposed at edge of highway, on right, at west end of bridge) by red, crossbedded, eolian sandstone. Davis Canyon Tuff is beneath the sandstone about 100 ft down-creek from the bridge. **0.1**

30.6 MP 5. Roadcut in Bearwallow Mountain Andesite. Cliffs of Bloodgood Canyon Tuff on both sides of canyon just beyond roadcut. **0.5**

31.1 **Slow**! Highway bridge over Starkweather Canyon. Beyond the bridge, in the bushes on the north (left) side of the road, coarse talus facies of the Gila Formation marks the trace of the Saliz Mountains-Higgins Mountain fault (Fig. 3.4), and we cross into Gila Formation on the hanging wall dip slope of the Jon S Mountain half graben tilted block (Jon S-Enid block of Crews, 1990). This coarse, angular talus deposit is a typical colluvial wedge of Gila Formation facies association no. 5 (Crews, this volume), adjacent to an intrabasin fault scarp. **0.4**

31.5 Reserve Ranger Station on right. MP 6 just ahead. **1.0**

32.5 Junction in downtown Reserve. **Turn left with NM-12.** The road to the right follows the San Francisco River valley south for about 7 mi, where the Bloodgood Canyon Tuff, in the deepest part of the Reserve graben, is at river level at about 5600 ft elevation at the southern border of the Reserve quadrangle (J. C. Ratté, unpubl. 1989). The position of the Bloodgood Canyon there represents a drop of about 2625 ft from exposures near Alpine, Arizona, where this trip began.

East of the San Francisco River, here in the Reserve quadrangle, northeast-trending faults dip mainly northwestward, and provide some symmetry to the otherwise asymmetrical system of half grabens. The Keko Canyon fault, in the Milligan Mountain quadrangle (Ratté and Bove, in press, 1994) seems to mark a change from rotated fault blocks to a series of narrow, non-rotated blocks, by which the Bloodgood Canyon Tuff is re-elevated to an elevation of greater than 8000 ft on the east side of the Reserve graben, at the south end of the Tularosa Mountains. Thus, the Reserve graben system, from the Luna fault on the west to the vicinity of Eagle Peak to the east, is about 25 mi wide. **0.5**

33.0 Bridges across San Francisco River; continue north through roadcuts in Gila Formation, in the hanging wall slope of the Jon S tilted block. **0.9**

33.9 Cross east boundary of Reserve quadrangle into Milligan Mountain quadrangle (Ratté and Bove, in press, 1994). Views to east (right) of the south end of the Tularosa Mountains (Fig. 3.9) on the east side of the Reserve graben. Eagle Peak is the central vent for the 11-12 Ma dacitic Eagle Peak volcano, and Milligan Mountain is a satellitic eruptive center (see following minipaper by Bove, et al).

To the west is the Higgins Mountain half-graben tilted block; meanwhile we are crossing the dip slope of the Jon S half graben, the next rotated block to the east. The Saliz Mountains-Higgins Mountain fault, along the base of Higgins Mountain, separates the two half grabens (Fig. 3.10). Fine-grained Gila Formation adjacent to the fault is among the finest-grained beds observed in the Reserve area, and is interpreted as axial-fluvial facies deposited along the fault, and it contrasts with the coarser-grained, dip-slope canyon-fill facies and distal fan deposits in the roadcuts that we have just driven through. Note the broad syncline in Gila beds along the Saliz Mountains- Higgins Mountain fault (Fig. 3.10). The syncline may indicate some strike-slip component of movement along this fault. The San Francisco River enters valley through the San Francisco Box, where it has cut through flows of the andesite of Dry Leggett Canyon at about 11 o'clock. **1.2**

35.1 Junction, road to Eagle Peak. **Turn right (east).** Between this junction and Tularosa river ahead, we are crossing the Jon S tilted block. Jon S Mountain consists of the two cuesta ridges east of NM-12 and north of the Eagle Peak road. The local volcanic stratigraphic sequence is largely repeated by a fault between the ridges. Along this part of the Eagle Peak road, we are crossing Gila Formation and alluvium. **0.5**

THE EVOLUTION OF THE MID-TERTIARY EAGLE PEAK VOLCANO, CATRON COUNTY, NEW MEXICO

Dana J. Bove[1], James C. Ratté[1], William C. McIntosh[2], Lawrence W. Snee[1], and Kiyoto Futa[1]

[1]U.S. Geological Survey, Denver, CO 80225;
[2]New Mexico Bureau of Mines and Mineral Resources, Socorro, NM 87801

Eagle Peak is a well-preserved, low-angle, calc-alkaline volcano in the mid-Tertiary Mogollon-Datil volcanic field of southwestern New Mexico. Geologic mapping (Bove et al., 1989; Bove, 1990), in conjunction with petrologic studies allows the differentiation of several distinct andesitic to dacitic eruptive phases (Fig. 3.11). These phases can be subdivided into either central vent or satellitic facies, depending on the site of eruption or emplacement. The central vent series includes andesitic to dacitic flows, agglomerate vent breccias, and a dacitic plug, whereas the

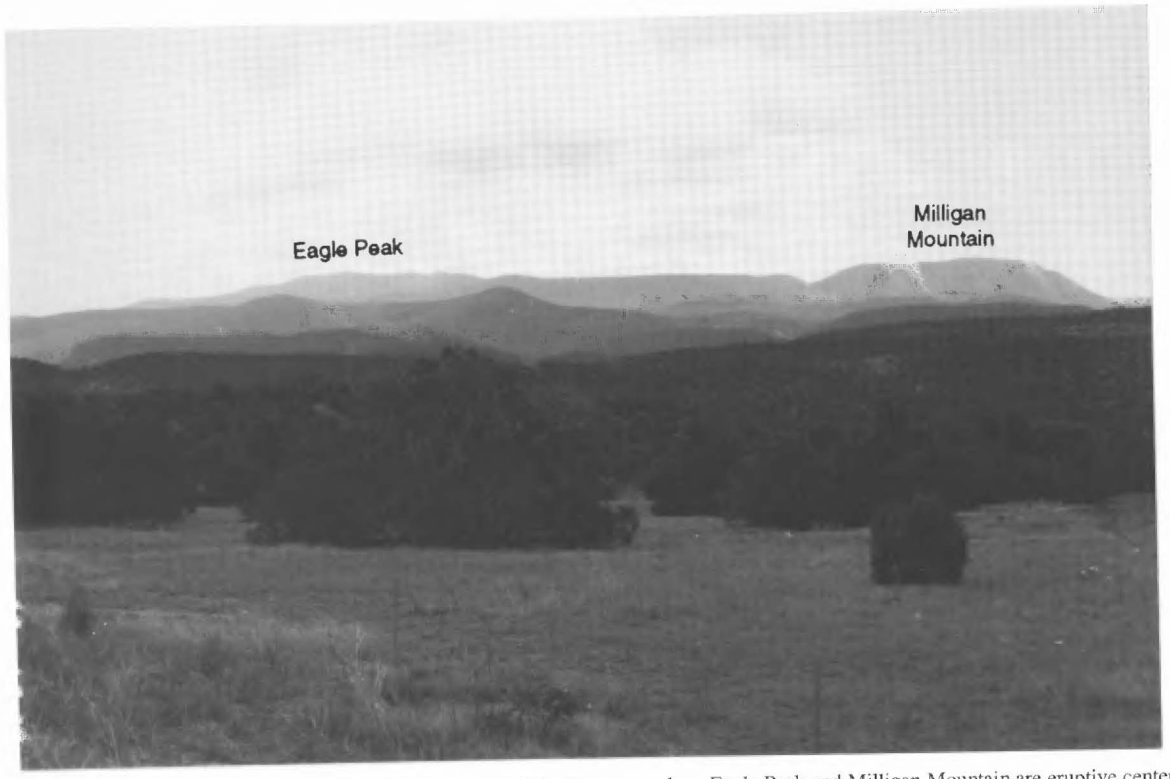

FIGURE 3.9. View east (to right) to Tularosa Mountains on the east side of the Reserve graben. Eagle Peak and Milligan Mountain are eruptive centers of the 11-Ma Eagle Peak dacite (see Bove and Ratté, this volume).

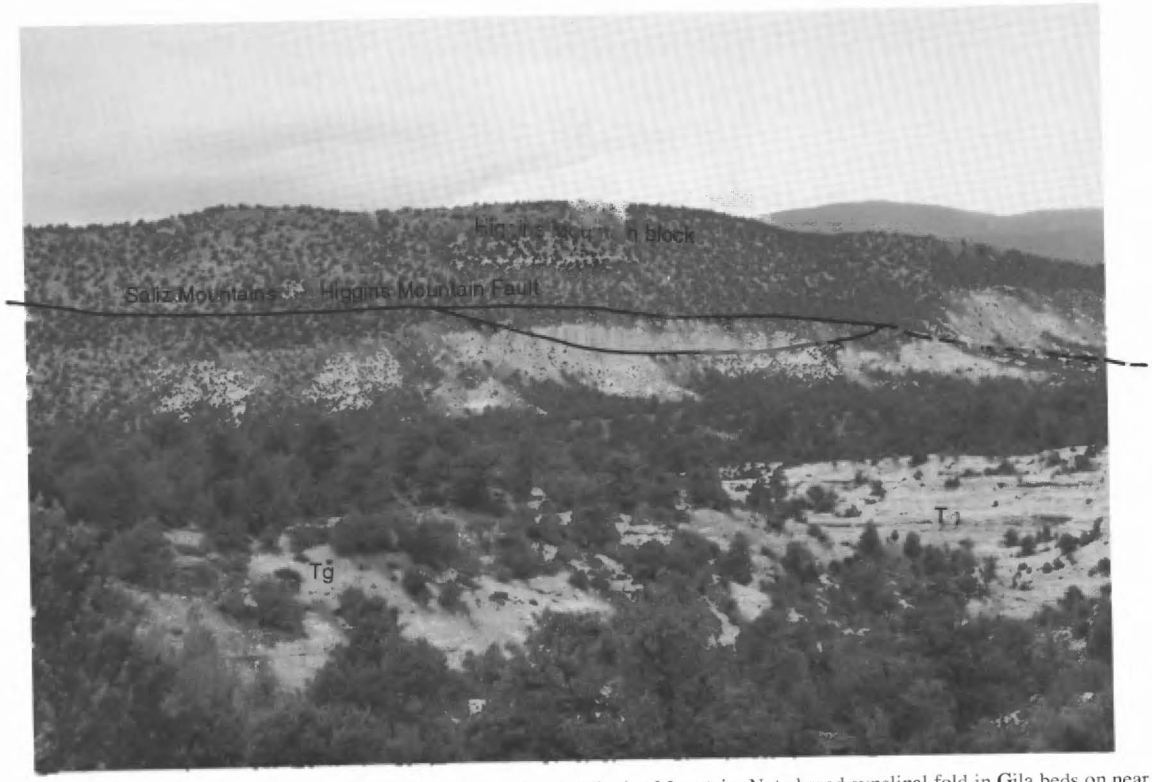

FIGURE 3.10. View west from NM-12 across dip slope of Gila Formation, Tg, to Higgins Mountain. Note broad synclinal fold in Gila beds on near side of Higgins Mountain fault; fold may be an indication of at least some strike-slip component on the fault.

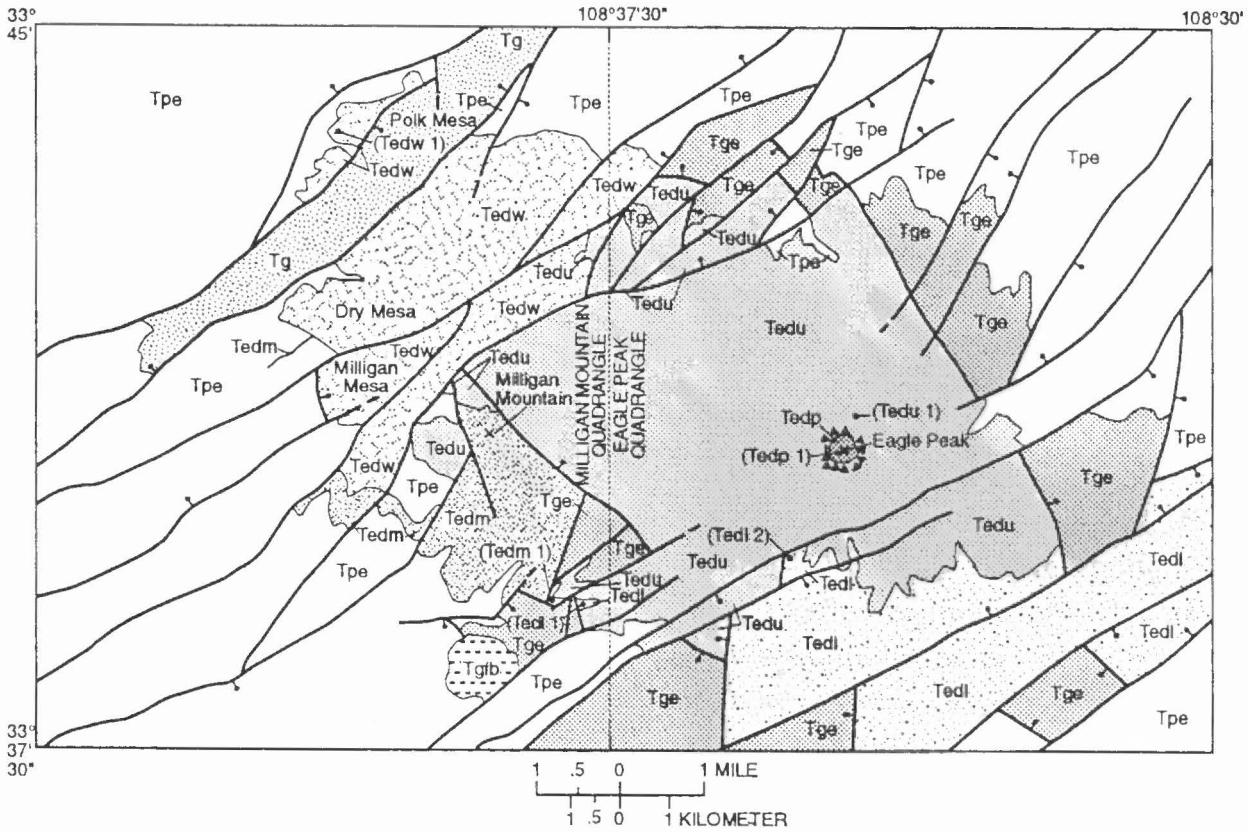

CORRELATION OF MAP UNITS

(Ages cited besides boxes; Ma is Mega-annum (10^6 years); R or N beside boxes or following ages indicates reverse or normal magnetic polarity, respectively; numbers in parenthesis following age or polarity indicate reference to age or paleomagnetic data as follows: this study, Ratte' and others, in press)

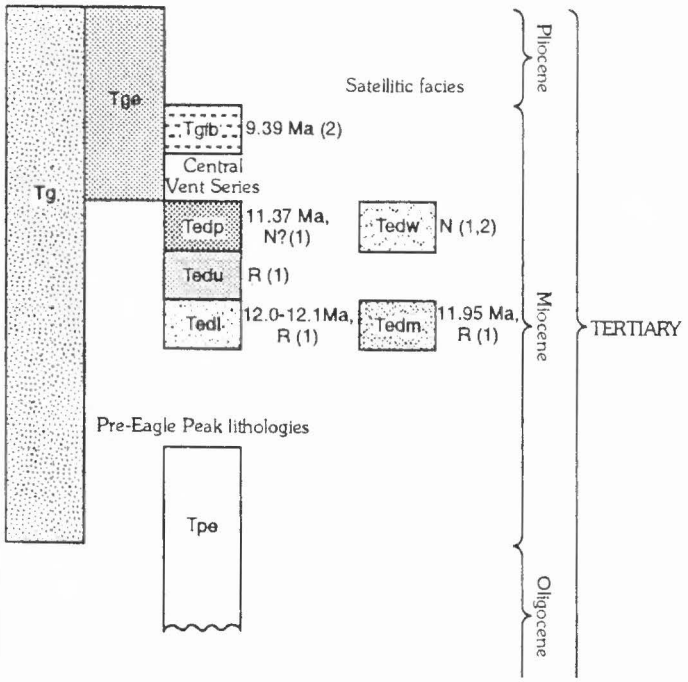

EXPLANATION

GILA FORMATION

- Tg — Sedimentary rocks, undivided (Pliocene and Miocene)
- Tge — Eagle Peak volcaniclastic beds (Pliocene and Miocene)
- Tgfb — Basalt on Flat Top Mesa (Miocene)

DACITE OF EAGLE PEAK (MIOCENE)

Central vent facies

- Tedp — Dacite porphyry plug
- Tedu — Upper Eagle Peak flow rocks
- Tedl — Lower Eagle Peak flow rocks

Satellitic facies

- Tedw — Wilson Canyon flow rocks
- Tedm — Milligan Mountain flow rocks

OLDER ROCKS

- Tpe — Pre-Eagle Peak rocks, undivided (Tertiary)

SYMBOLS

- Contact
- Fault—Ball and bar on downthrown side
- Agglomerate breccia
- (Tedl 1)— Sample number and locality for paleomagnetic data and (or) $^{40}Ar/^{39}Ar$ age

FIGURE 3.11. Geologic map of Eagle Peak Volcano area, Catron Country, New Mexico.

satellitic facies consists of thick andesitic flows and a feeder dike. Lavas erupted from the central vent area are separated into upper (Tedu) and lower (Tedl) flow units; upper flows are distinguished from lower flows by the low percentage of phenocrysts, absence of hydrous mineral phases and ilmentite, and more evolved compositions. Satellitic flows comprise two distinct bodies of lava erupted from centers on the western (Milligan Mountain unit, Tedm) and northwestern (Wilson Canyon unit, Tedw) margins of the volcano (Fig. 3.11). The Milligan Mountain and Wilson Canyon satellitic lavas, although chemically indistinguishable, are petrographically different. Milligan Mountain lavas contain a hydrous mineral-bearing assemblage, similar to that of the upper unit central vent flows, whereas Wilson Canyon lavas are essentially anhydrous but contain enclaves of finely porphyritic andesite (?) containing disequilibrium hornblende.

$^{40}Ar/^{39}Ar$ and paleomagnetic studies indicate that the Eagle Peak volcano was active between 12.1 and 11.4 Ma (Ratté et al., in press) and spanned at least one reversal in magnetic polarity. A weighted mean age of 11.73 ± 0.04 Ma was calculated for the reversely magnetized central vent and Milligan Mountain satellitic flows using the inverse of the sample error or variance (Taylor, 1982). These ages were averaged because they are analytically indistinguishable at the 95% confidence level, and geologic and paleomagnetic data indicate that flows represented by these samples were emplaced in rapid succession. The weighted mean age of 11.73 Ma, which takes into account the accuracy of the individual analysis, is analytically distinguishable at the 95% confidence level from the 11.37 ± 0.09 Ma central plug (Tedp). Geologic and petrogenetic constraints suggest that the normally magnetized Wilson Canyon lavas formed very late in the Eagle Peak volcanic sequence.

Major oxide, trace-element, and isotope geochemistry indicates that the central vent and satellitic eruptives define two separate and distinct magmatic series. The satellitic series, although similar in modal mineralogy and REE patterns to the central vent series, is slightly more alkaline and relatively enriched in the high field strength elements Nb, Ta, P and Ti. Satellitic series rocks ($^{87}Sr/^{86}Sr_i$ =0.70839, ∈Nd =-4.8) also show less upper crustal contamination and are probably more primitive than rocks of the central vent series ($^{87}Sr/^{86}Sr_i$ =0.70958, ∈Nd =-8.5).

Constraints based on major and trace element data support petrogenetic models that require a periodic tapping of the central vent and satellitic series magmas, which individually became more evolved by removal of crystals from the magma chamber. Crystal fractionation modelling of the central vent series suggests that magma forming the hydrous lower unit lavas was parental to the anhydrous upper unit flows. Accordingly, initial eruptions (62-64% SiO_2) from the central vent tapped a deep level magma reservoir in which hydrous mineral phases and ilmentite were stable. Subsequent anhydrous central vent eruptions (64-67% SiO_2) tapped a higher level reservoir that was established after eruption from the deep reservoir. The upper level reservoir was probably fed repeatedly from the deeper magma chamber. Transfer of magma into the shallow reservoir favored conditions of lower P_{H2O} and fO_2 resulting in the destabilization of the hydrous mineral phases and ilmentite, respectively. This scenario is supported by the rare occurrence of disequilibrium hornblende in the otherwise anhydrous upper unit and the presence of magnetite without ilmentite, which are present together in the lower unit. The near uniformity in parent-daughter orthopyroxene and plagioclase core compositions in the upper unit is consistent with a system in which the bulk magma chemistry evolved mainly by crystal removal without evolution in the major phenocrysts or in the residual magma. In contrast, least-squares modelling results paired with the presence of evolving phenocryst compositions within rocks of the satellitic series suggest that the residual magma evolved in conjunction with crystal fractionation.

Regionally, the Eagle Peak volcanic rocks, although temporally associated with <21-Ma bimodal basalt-rhyolite volcanism (Group II of Ratté and Futa, 1989), have strong geochemical affinities for Group I rocks of Ratté and Futa (1989), which mainly consist of 27-23 Ma-Bearwallow Mountain Andesite. Sr and Nd isotope chemistry demonstrates that Group II mafic rocks, which have Sr and Nd isotopic ratios ranging from depleted mantle to bulk earth values ($^{87}Sr/^{86}Sr_i$ = 0.7030-0.7057, ∈Nd = 0 to +9.12), are substantially more primitive than Eagle Peak rocks ($^{87}Sr/^{86}Sr_i$ = 0.70839-0.70958, ∈Nd =-8.5 to -4.8). In contrast, Eagle Peak rocks are geochemically more similar to Group I Bearwallow Mountain rocks ($^{87}Sr/^{86}Sr_i$ = 0.7070-0.7102, ∈Nd =-8.15 to -5.95). Eagle Peak and Group I volcanic rocks are strongly depleted in the HFS elements relative to Group II rocks and are enriched by two to four times in the elements Rb, Zr, Ba, Th and Hf. Eagle Peak rocks and Group I andesites were affected significantly by upper crustal contamination and were probably derived from similar magmatic sources.

35.6 Crossing Largo Creek; views to left of Jon S composite fault block, with 20-25° dip slopes on the two fault-separated hogbacks (Fig. 3.12). **0.8**

36.4 Road crosses crest of low north-south ridge capped by Group II "true" basalt of Futa and Ratté (1989, p. 100) as distinguished from older, contaminated mafic rocks such as the Bearwallow Mountain Andesite, Group I of Futa and Ratté. Basalt barely crops out beyond side trail on left, and as a dark patch on right side of road, but caps ridge on north (left) side of road for 0.6-1.2 mi. An Ar/Ar age of ~ 13.7 Ma has been determined for plagioclase from this flow. These young Group II basalts are associated with basin- and- range extensional faulting around the margins of the Mogollon-Datil volcanic field.

The Group II basalts also are sometimes described as "big feldspar" basalt because they commonly contain plagioclase phenocrysts 0.4-1.2 in. or larger (Figs. 3.13, 3.14). The clarity and citrine yellow color of the plagioclase phenocrysts make them much prized by "rockhounds" as semi-precious stones, which are known popularly and sold commercially as "bytownite" (Murphy, 1971), and are commonly faceted for rings and other jewelry. However, the feldspar crystals are actually labradorite (An 67-68), as indicated by their refractive indices and x-ray pattern. Some centimeter-size phenocrysts have been found near here, but much better collecting can be found elsewhere, as in the Saliz Pass quadrangle (Ratté, 1980). **0.8**

37.2 Sharp switchback to left. Tuff of Triangle C Ranch, a few meters thick, exposed at left edge of road, about 300 ft beyond curve. This tuff, which is indistinguishable in age and composition from the Bloodgood Canyon Tuff, is distinct in having normal paleomagnetic polarity, and locally, as here, is separated from the underlying Bloodgood Canyon Tuff (28.1 Ma) by a few feet of volcaniclastic sedimentary rock. **0.2**

37.4 Outcrops on left side of road at river level were mapped as Bearwallow Mountain Andesite because they lack the big feldspar phenocrysts characteristic of the younger basalt flows, but their relatively fresh appearance, abundance of fresh olivine, and microdiabase texture suggest that they may, in fact, be the younger basalt. See further discussion in the following minipaper.

Gila Formation outcrops ahead are faulted down by the east-northeast-trending Kimball Spring fault (Fig. 3.12); Bloodgood Canyon Tuff and older rocks form the footwall behind the fault, to the ridge crest. The Gila Formation here is the prime example of Crews' (1990) facies association 4, massive, channeled sandstone (see Crews, this volume, fig. 10). **0.2**

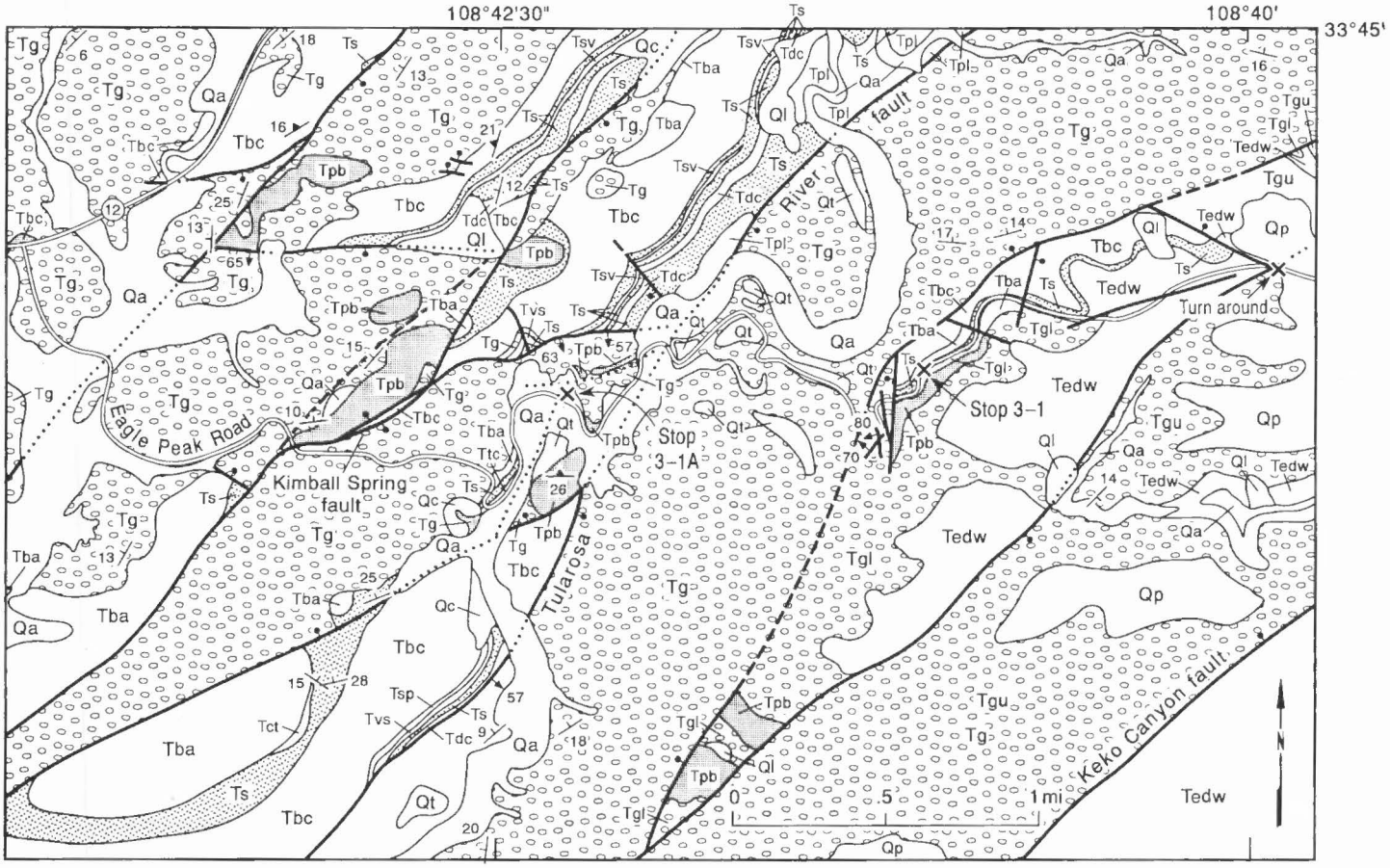

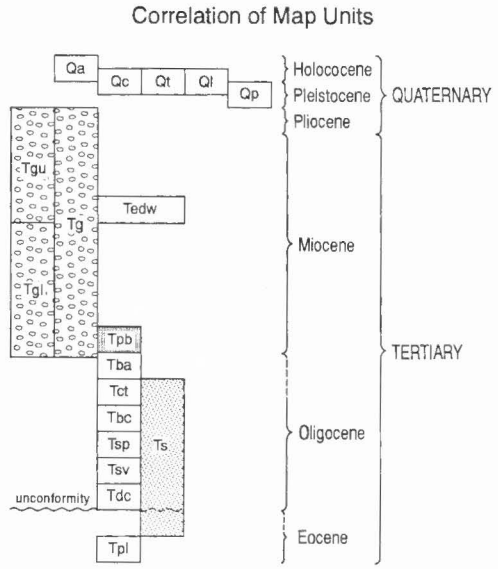

Map Units

Surficial Deposits (Quaternary)
- Qa—alluvium
- Qc—colluvium and talus
- Ql —landslide deposits
- Qt —terrace gravels
- Qp—pediment gravels

Gila Formation (Pliocene–Oligocene)
- Tg —Gila Formation undivided
- Tgu—Upper Gila Formation (Pliocene and Miocene)
- Tgl —Lower Gila Formation (Miocene and Oligocene)

Tedw— Eagle Peak dacite (Miocene)
Tpb — Basalt of Pueblo Park (Miocene)
Tba — Bearwallow Mountain Andesite (Miocene and Oligocene)
Tct — Tuff of Triangle C Ranch (Oligocene)
Tbc — Bloodgood Canyon Tuff (Oligocene)
Tsp — Shelley Peak Tuff (Oligocene)
Tsv — Squirrel Springs Canyon Andesite and/or Vicks Peak Tuff (Oligocene)
Tdc — Davis Canyon Tuff (Oligocene)
Ts — Spears Group volcaniclastic sedimentary rocks (Oligocene and Eocene)
Tpl — Dry Leggett andesite (Eocene)

FIGURE 3.12. Geologic map of the Jon S half graben in the vicinity of Stop 1. Adapted from Ratté and Bove (1994).

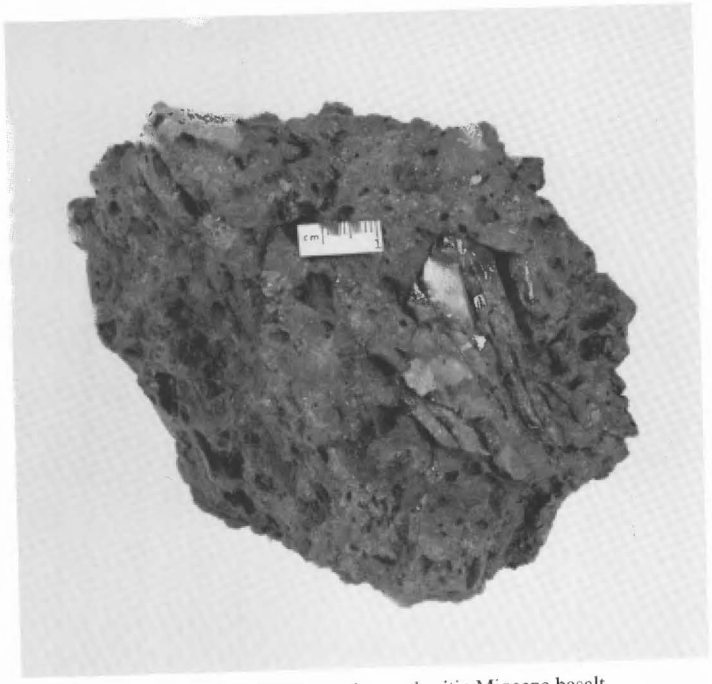

FIGURE 3.13. Labradorite megacryst in porphyritic Miocene basalt.

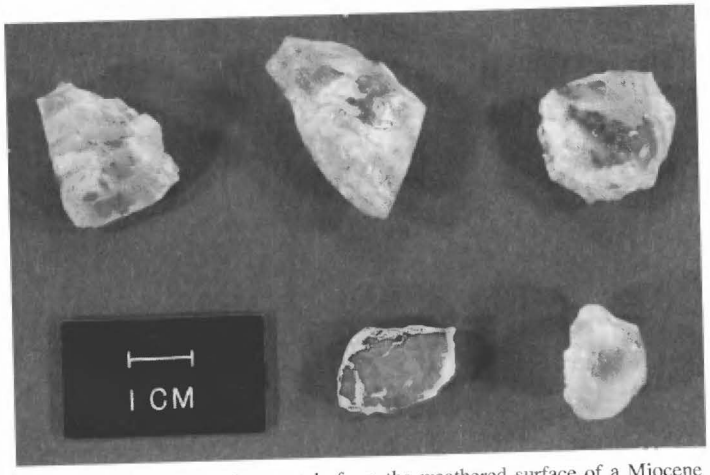

FIGURE 3.14. Labradorite crystals from the weathered surface of a Miocene basalt flow in the Saliz Pass quadrangle southwest of Reserve (Ratté, 1980).

DISTINGUISHING YOUNG 'TRUE' BASALTS FROM BEARWALLOW MOUNTAIN ANDESITE

J.C. Ratté, D.J. Bove and Kiyoto Futa

U.S. Geological Survey, P.O. Box 25046, MS 905, Denver, CO 80225

Distinguishing Basin-and-Range-age basalt (group II) and largely pre-Basin-and-Range-age Bearwallow Mountain Andesite (group I) can be a difficult mapping problem. In most outcrops, the relatively fresh appearance and the presence of large but generally sparse plagioclase and augitic pyroxene phenocrysts, or interlayering with Gila Formation sedimentary rocks serve to identify the group II basalts of Futa and Ratté (1989) from older group I basaltic andesite to dacitic flows of Bearwallow Mountain Andesite. Major oxide and trace element analyses usually provide clear distinctions between the two groups, but not always. The use of zirconium:niobium ratios or Zr:Nb plotted against SiO_2 contents, can be useful in distinguishing the mafic flows of the two groups, but it also has its limitations. Most group I basalts have Zr:Nb ratios greater than 10, and most group II rocks have Zr:Nb less than 10, but some rocks that have Zr:Nb in the 8-12 range are ambiguous. Rb-Sr and Sm-Nd isotope analyses also tend to separate these mafic rocks into two distinct groups in most cases, and provide evidence of different magmatic source regions related to the structural evolution of the Mogollon-Datil region (Futa and Ratté, 1989).

The recognition problem is well illustrated in the vicinity of Kimball Spring in the Milligan Mountain quadrangle near Stops 1 and 1A. Four outcrops of mafic lava flows, labelled 1-4 on Figure 3.12, were mapped as either group I or group II on their field characteristics, and then sampled for chemical comparisons (Table 3.1). The rocks at localities 2 and 4 were identified as young basalts during mapping, whereas the flow at locality 3 was mapped as Bearwallow Mountain Andesite; their distinguishing lithologic characteristics are consistent with stratigraphic sequence. At locality 1, however, where the geologic context favors correlation of the outcrops on opposite sides of the river, the mafic flow east of the river is easily identified as belonging in group II by its sparse, big plagioclase phenocrysts, but the flow along the road at locality 1, west of the river, gives mixed signals. It seems to lack large plagioclase phenocrysts, and it has a Zr:Nb ratio of 12, nearly identical to that of the Bearwallow Mountain Andesite sample from locality 3 (Table 3.1); these characteristics imply a group I affinity. However, the bulk chemistry of the rock at locality 1 (Table 3.1), shows a basaltic composition, with SiO_2 content intermediate between that of group II samples from localities 2 and 4; the highest MgO and CaO, by far, of any of the four samples, and the lowest K_2O of the four samples, all indicating a more likely affinity for the young basalts of group II. Additional chemical analyses or dating, or both, will be necessary to ascertain if the Bearwallow Mountain Andesite mapped at locality 1 on the published map (Ratté and Bove, in press) is correctly identified.

37.6 Cross cattleguard. Corrals on left. Return here later and park for Stop 1A. **0.3**

37.9 Sharp curve with young, "big feldspar" basalt outcrops on left. This is locality 2 on Figure 3.12 and in Table 3.1. Basalt contains 0.4-0.8 in. labradorite, and 0.2-0.4 in. augite phenocrysts, and quartz-diorite? crustal xenoliths. **0.3**

38.2 Ford across Tularosa River above Kimball Spring. Jon S tilted block to west, with Kimball Spring-Tularosa River volcanic sequence exposed in slopes above river. Road now crosses through Gila Formation between Tularosa River fault, at river level, and unnamed fault to east (Fig. 3.12). Unnamed fault defines the west side of a narrow, wedge-shaped horst within the also wedge-shaped, symmetrical, Tularosa graben, which is at the eastern footwall of the Reserve graben, marked by the Keko Canyon fault. **0.9**

39.1 Road is now on uppermost of three Tularosa River terraces, here on the east side of the river. As road curves to right, approaching fault on west side of intragraben horst, view through opening in trees to left shows Bloodgood Canyon Tuff, at about this level within the horst. **0.2**

39.3 Switchback to left. Before turn, view is up Wilson Canyon, where Eagle Peak dacite flows (11-12 Ma) can be seen *overlying* lower Gila Formation. **0.4**

39.7 Curve overlooks big bend in Tularosa River. Roadcuts on right show young basalt above Gila Formation. **This is Stop 1, but continue to designated turnaround on mesa top. 0.2**

TABLE 3.1. Comparative chemical analyses of Bearwallow Mountain Andesite (Tba) and younger basalt of the bimodal basalt-rhyolite suite (Tb) in the vicinity of Stop 1. X-ray spectrography: laboratory chief, J.S. Mee; analysts, D.F. Siems and J.S. Mee. Zr and Nb by Ratté.

Map no. (Fig. 3-35.55)	1	2	3	4	5
Formation	Tb?	Tb	Tba	Tb	Tb
SiO_2*	50.5 (50.8)	50.8 (51.7)	51.9 (53.4)	49.8 (50.9)	54.9 (55.1)
Al_2O_3	15.4	16.2	14.5	16.6	17.4
$FeTO_3$	11.5	11.3	9.13	11.8	8.34
MgO	6.91	4.84	5.13	4.28	4.60
CaO	8.51	7.48	7.30	7.70	7.73
Na_2O	3.01	3.35	3.09	3.45	4.00
K_2O	1.20	1.81	3.23	1.67	1.71
TiO_2	1.90	1.94	1.73	2.04	1.35
P_2O_5	0.35	0.37	0.92	0.39	0.44
MnO	0.15	0.17	0.13	0.15	0.13
LOI (925°C)	0.41	1.66	2.44	1.99	0.31
SUM	99.84	99.92	99.50	99.87	100.01
Zr:Nb	12	5	13	5	5

*SiO_2 values in parentheses are normalized volatile free.

39.9 Bearwallow Mountain Andesite crops out along road; compare this fine-grained basaltic andesite, having tiny, orange, iddingsite-after-olivine grains, with the similar but coarser grained "big feldspar" basalt at the previous point. The Bearwallow Mountain Andesite here dips southward beneath the Gila Formation and younger basalt down the road. **1.1**

41.0 Road tops out on Polk Mesa. **Make U-turn, utilizing space off road to right, around tree.** Retrace route to overlook at Stop 1. Park along edge of road behind lead vehicle. **1.3**

42.3 **STOP 1.** The purpose of this stop is to present an overview of the Tularosa and San Francisco river valleys, as a basis for a discussion of the Reserve graben. This stop also affords an excellent view of the volcanic sequence present in the Jon S half graben block as exposed in the footwall of the Tularosa River fault on the west side of the river (Fig. 3.15). After a discussion of what you can see from here, and the regional context, we'll go down into the valley to Stop 1A and crawl around on the rocks a bit.

At this viewpoint, we are standing on a narrow horst within the deepest part of the Reserve graben. Behind us, about 1 mi to the east, is the westward-dipping Keko Canyon fault, along which stratigraphic units are uplifted eastward within the Tularosa Mountains block on the eastern side of the Reserve graben. To the west, we are looking across the Tularosa River fault at the obsequent face of the Jon S Mountain tilted block. Here, along the road, thin Bearwallow Mountain Andesite flows overlie thin volcaniclastic sandstone, which is above Bloodgood Canyon Tuff in the slopes below us. The fault on the west side of this narrow horst drops the Gila Formation down to river level. However, deposition of the Gila beds, according to the half-graben model presented here for the Reserve graben system, accompanied rotational (listric) faulting and was confined to individual basins within the half graben, at least initially (Crews, 1990). On the slopes above us, on the east side of the road, thin Gila Formation is overlain by thin, young, basalt flows, more Gila beds, and dacite flows of Eagle Peak from the Eagle Peak volcano in the Tularosa Mountains to the east (Fig. 3.12).

The volcanic sequence exposed across the Tularosa River (Fig. 3-15) consists of the following units: at river level, barely visible from here, are porphyritic flows of red-gray andesite of Dry Leggett Canyon (~ 34 Ma), overlain by mostly red volcaniclastic sedimentary rocks about 525 ft thick, of the Oligocene Pueblo Creek Formation (Ratté, 1989), which is now included in the Eocene and Oligocene Spears Group. Above, are the approximately 100 ft-thick, bold, columnar jointed cliffs of 29-Ma Davis Canyon Tuff, which was erupted from the Mogollon Mountains cauldron complex, in turn overlain by volcaniclastic sedimentary rocks and 16-33 ft of 28.6-Ma Vicks Peak Tuff, which was erupted from the Nogal Canyon cauldron at the south end of the San Mateo Mountains about 75 mi to the east. The Vicks Peak Tuff is discontinuously overlain by 0-16 ft of Squirrel Springs Canyon Andesite. Above, is another 80-100 ft of volcaniclastic sandstone, capped by about 200 ft of 28.1-Ma Bloodgood Canyon Tuff, erupted from the Bursum caldera in the Mogollon Mountains about 12 mi to the southeast. The total thickness of the volcanic sequence as seen from here is about 1000 ft, and on top of that are patchy outcrops of Bearwallow Mountain Andesite and Gila Formation that mantle the dip slope, out of sight from here, on the back side of the ridge.

A down-to-the-south, high-angle normal fault offsets this sequence about 65-100 ft in the face of the Jon S block, and the much larger, east-northeast-trending Kimball Springs fault 1000-1300 ft to the left of the smaller fault, drops the Gila Formation down against

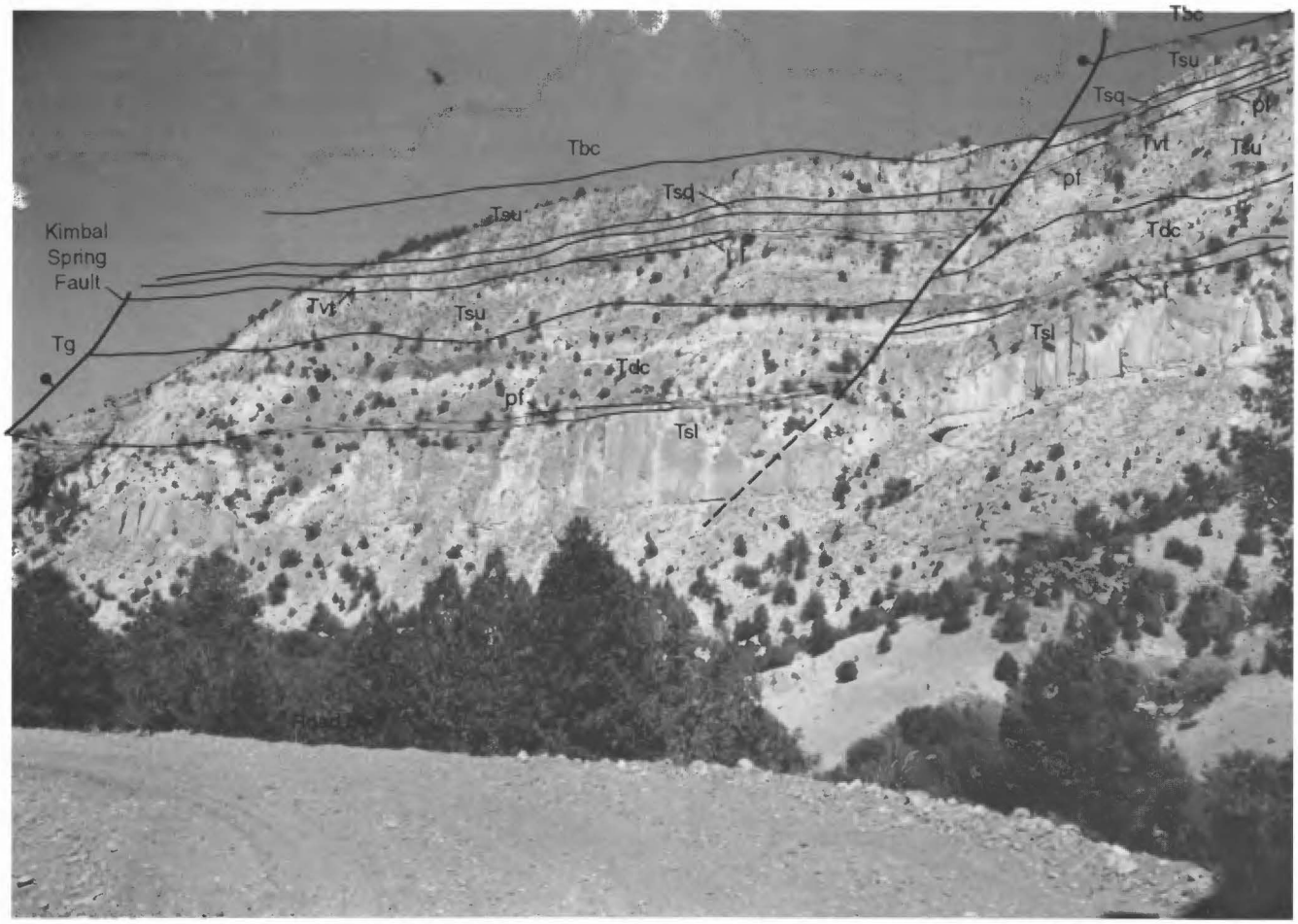

FIGURE 3.15. View of Kimball Spring volcanic sequence near Stop 1. **Tls**, lower Spears Group volcaniclastic rocks; **Tdc**, Davis Canyon Tuff (29 Ma) with 1-2 m of non-welded pyroclastic flow, **pf**, at base; **Tus**, upper Spears Group volcaniclastic rocks; **Tvt**, Vicks Peak Tuff (28.5 Ma) with a few meters of non-welded pyroclastic flows, **pf**, at base; **Tsq**, Squirrel Springs Canyon Andesite; **Tbc**, Bloodgood Canyon Tuff (28 Ma).

the volcanic sequence. This east-northeast-trending Kimball Springs fault links the Tularosa River fault and the next northeast-trending graben fault to the west, which offsets the two Jon S Mountain ridges.

Looking to the southwest, down the Tularosa River valley (Figs. 3.16, 3.17) we see the double, west-dipping cuestas with the saddle between, which constitute the continuation of the Jon S block (Fig. 3.15). To the right of the double cuesta, the ridge with the open areas along its base is the Saliz Mountains tilted block on the west side of the San Francisco River. The Saliz Mountains block is the southward continuation of the Jon S and Higgins Mountain sub-blocks, which lose their identity south of Starkweather Canyon, which can be seen at the break in slope at the north end of the Saliz Mountains ridge. The next ridge to the west, on the skyline, is the San Francisco Mountains on the west side of the San Francisco Mountains fault zone. On a clear day, the stretch of US-180 that is on the east side of Mail Hollow divide near the Heifer Basin overlook (Fig. 3.6) can be seen from here.

The Reserve graben has been known as a major structural feature at least since the reconnaissance geologic map of the Reserve 30-minute quadrangle (Weber and Willard, 1959). It was described as one segment of the outer graben system surrounding the Mogollon plateau, which has been interpreted as the surface expression of a large composite pluton about 75 mi in diameter (Elston et al., 1976), and a genetic relationship between the graben system and the batholith has been implied. Recent, detailed USGS geologic mapping of 7-1/2 minute quadrangles along the Morenci-Reserve fault zone, including the Reserve graben, has led to the proposal that the Reserve graben is actually part of a separate structural trend (~ N35°E), more northerly than the Morenci lineament (~ N55°E), which includes the San Agustin graben (Ratté, 1989). It has been speculated that the N35°E Morenci-Reserve trend might extend northward beyond the Reserve area, possibly intersecting the N52°E Jemez lineament (Aldrich et al., 1981; Aldrich and Laughlin, 1984) in the vicinity of Mount Taylor (Futa and Ratté, 1989), rather than bending around the north end of the Mogollon plateau, as proposed by Elston et al. (1976). Reconnaissance geologic mapping of the Quemado 1:100,000 quadrangle by Chamberlin et al. (1994b), has reinforced the idea that the Morenci-Reserve fault zone extends northward as

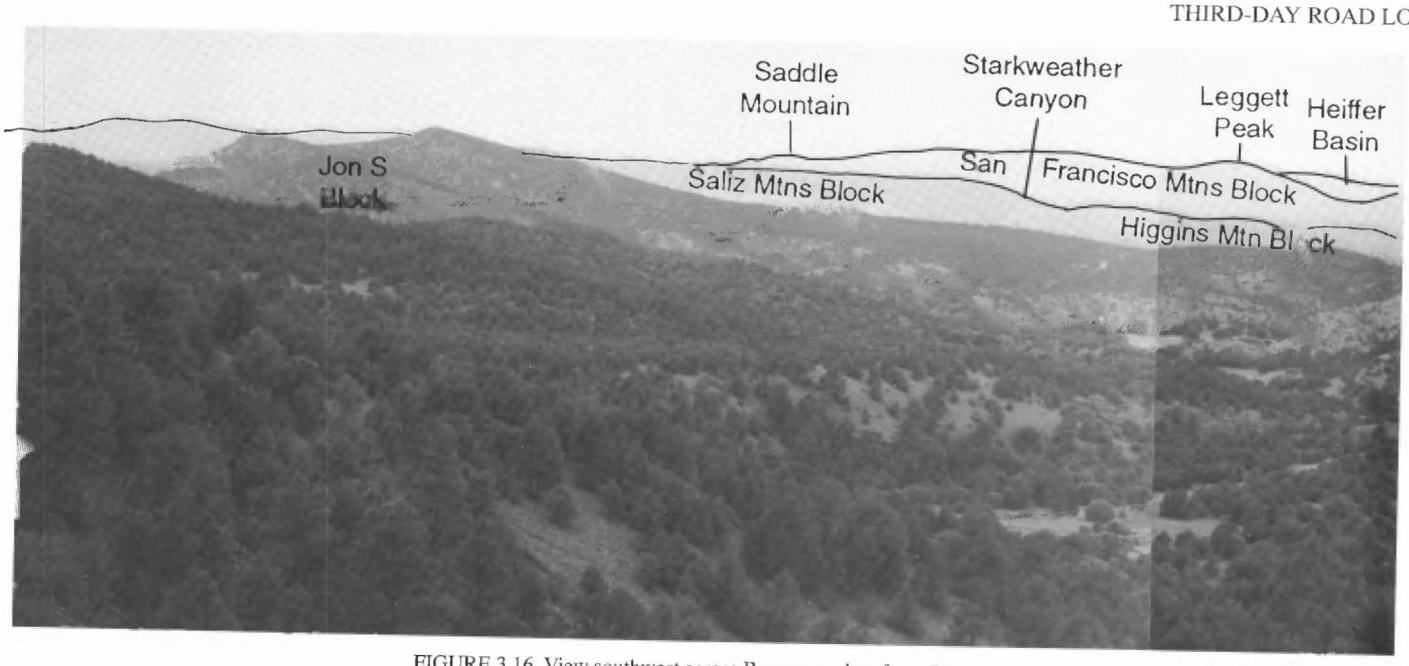

FIGURE 3.16. View southwest across Reserve graben from Stop 1.

represented by the Hickman and Spur Lake faults discussed in the Day 1 road log of this volume.

In summary, the Reserve graben, or graben system, is considered to be about 25 mi wide between the Luna fault on the northwest side and the Keko Canyon fault on the southeast side. Bloodgood Canyon Tuff, the 28-Ma outflow sheet of the Bursum caldera, was downdropped from an elevation of about 8000 ft or more, near Alpine about 15 mi west of Luna, to about 5500 ft elevation along the San Francisco River south of Reserve, and was uplifted back to more than 8000 ft again in the Tularosa Mountains near Eagle Peak (Bove, 1990), 5-6 mi east of the Keko Canyon fault (Fig. 3.12). Thus the aggregate stratigraphic throw across the graben system is about 2625 ft.

The current structural interpretation of the Reserve graben as a series of tilted half grabens formed by rotation on shallow normal faults that flatten with depth is an outgrowth of the work of R.M. Chamberlin, C.E. Chapin, G.R. Osburn and S.M. Cather et al. on structures along the Rio Grande rift, and the northeastern part of the Morenci lineament in the vicinity of Socorro. Crews applied modern concepts of sedimentology and listric faulting specifically to the Reserve graben (Crews, 1990; this volume).

An additional regional aspect of the north-northeast Morenci-Reserve zone is its apparent segmentation by nearly east-west-trending oblique transfer(?) faults, such as the Kimball Springs fault. One of these east-west zones breaks the dip slope of the San Francisco Mountains block and appears to coincide with a dextral offset of the San Francisco Mountains fault zone (Fig. 3.4). Another east-west zone, the Sand Flat graben, marks a similar dextral offset of structure at the north end of the Tularosa Mountains near Aragon, but somewhat diminished north-northeast structures continue to the north into the Quemado 1:100,000 quadrangle. The full meaning of the fault pattern is currently unknown.

Return to cars and continue retracing route to ford across Tularosa River, and 0.4 miles beyond to optional stop 1A. 2.1

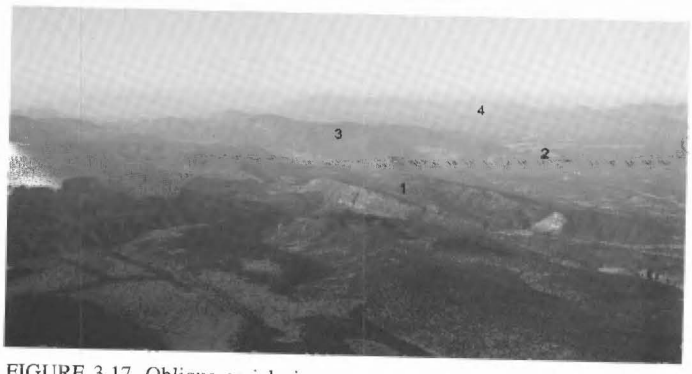

FIGURE 3.17. Oblique aerial view across the Reserve graben showing the major tilted fault blocks: 1, Jon S Mountain block; 2, Higgins Mountain block; 3, Brushy Mountains-Saliz Mountains block; 4, San Francisco Mountains block. R, Reserve.

44.4 **OPTIONAL STOP 1A**. At this stop we will examine a small-scale buttress unconformity and a small related reverse fault within the Gila Formation. But first, notice the changing dip of the Gila beds from sub-horizontal near the Kimball Springs fault to 10-15° or more east of the fault. Do these changing dips represent decreasing rotation of younger beds, or drag on the Kimball Springs fault? If the change in dip is related to drag, then the Gila beds in this place have been faulted and are not merely deposited against a preexisting fault scarp.

From the parking area, walk about 600 ft northeast to a small gulch where basalt on the west side is in contact with Gila on the east side, along an apparent fault contact, but Gila on the ridge crosses the projected

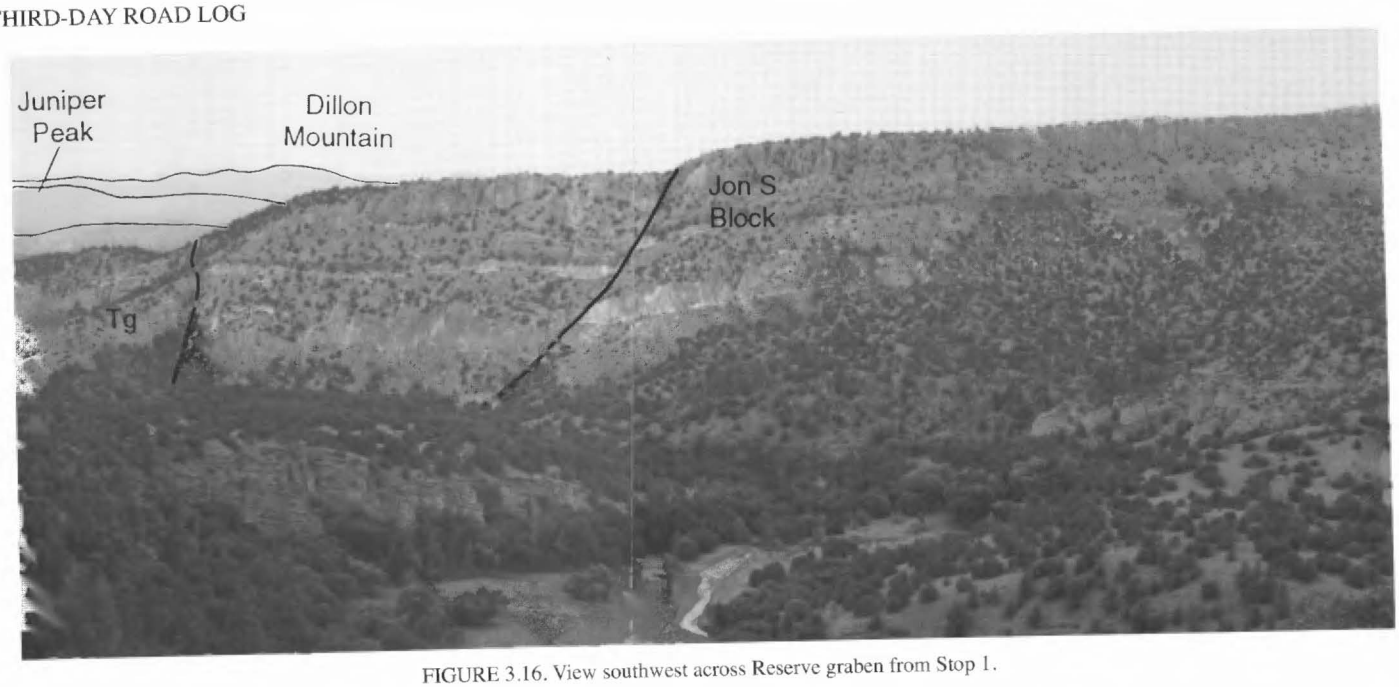

FIGURE 3.16. View southwest across Reserve graben from Stop 1.

trace of the fault without offset. Closer examination of the Gila-basalt contact shows basalt blocks included in the Gila along the contact, and thus it appears that this is a buried fault scarp that shed basalt cobbles into Gila beds that overlap basalt on the ridge crest without offset, thus a buttress unconformity. Observe the small reverse fault in the Gila Formation (Fig. 3.18) in the "hanging wall" of this outcrop, where the Gila beds have been deformed, but barely offset, during renewed movement on the buried fault.

From the parking area for stop 1A, one can walk back along the road about 1000 ft to the east and examine outcrops of young, "big feldspar" basalt (locality 2, Fig. 3.12; analysis 2, Table 3.1), at the point of the low ridge, at road level. After returning to stop 1A, walk south along the road about 1600 ft to examine outcrops of Bearwallow Mountain Andesite or young basalt (locality 1, Fig. 3.12; analysis 1, Table 3.1) for comparison. What would you call this outcrop? See specimens at parking area.

If time permits, some may wish to climb around to the Kimball Springs fault to see the oblique slickensides and look at some of the rocks in the older part of the volcanic sequence.

Return to cars and back-track to NM-12. 2.3

46.7 Junction of Eagle Peak road and NM-12. **Turn right on NM-12.** Directly opposite junction is a roadcut in young basalt, which is interlayered in the Gila Formation (see analysis 5, Table 3.1). Bove obtained a whole rock, Ar/Ar age of 13.5 ± 0.12 Ma on this basalt, nearly identical to the age of 13.7 Ma for the big feldspar basalt on the ridge crest to the east at mile 36.4. After right turn onto NM-12, Gila Formation in roadcut on right dips beneath young basalt opposite Eagle Peak road. **0.5**

47.2 MP-10. Bridge across Largo Canyon; outcrops ahead on right are typical densely welded Bloodgood Canyon Tuff on about 15° dip slope in hanging wall of Jon S Mountain block. Bloodgood Canyon Tuff here was called Railroad Canyon Rhyolite Tuff by Elston and Damon (1970, p. 140), with a suggested origin in the Corduroy Canyon cauldron in the Black Range (Elston, 1984, table 1). All Railroad Canyon Rhyolite Tuff is now correlated with Bloodgood Canyon Tuff (Ratté et al.,1984; McIntosh et al., 1991), and the name was abandoned by Lawrence and Richter, 1986. The Corduroy Canyon cauldron is no longer necessary, because the distribution of Railroad Canyon Rhyolite Tuff was the only evidence of its existence. Gila conglomerate unconformably overlies Bloodgood Canyon Tuff locally on this dip slope, and provides good examples of the dip-slope canyon-fills in the coarse proximal deposits of Crews' (this volume) facies association 1. **0.6**

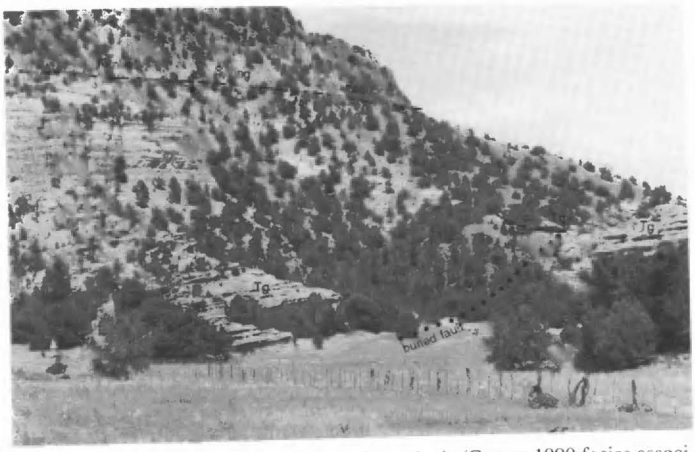

FIGURE 3.18. Massive, channelled sandstone beds (Crews; 1990 facies association 4) of Gila Formation, Tg, in hanging wall of Kimball Springs fault. Gila beds on right are deposited against faulted young basalt in a buttress unconformity. Tbc = Bloodgood Canyon Tuff.

47.8 North edge of Milligan Mountain quadrangle; entering Cruzville quadrangle (T.L.Finnell, unpubl., 1989). **0.4**

48.2 MP 11. Ahead, in roadcut on right, young basalt (Zr:Nb =5) overlies red, oxidized Gila Formation. **1.0**

49.2 MP 12. Ahead, 0.2 mi on left, junction with J.T.S.Park-Torriette Lakes road.

50.2 MP 13. Through trees on right, young (Miocene) basalt flow and underlying Gila Formation dip conformably about 15-20° to west toward highway. Crossing Jon S Flat between here and Cruzville, at MP 16, the hogback ridges east of the highway expose both basalt flows that dip conformably with the underlying volcaniclastic rocks, and younger, flat-lying basalt that unconformably overlies tilted Gila Formation sedimentary rocks, interlayered Miocene basalt, Bearwallow Mountain Andesite and Bloodgood Canyon Tuff. The flat-lying basalt probably all correlates with the basalt flow at Apache Creek, which has been dated at about 1 Ma (Bikerman, 1972; Marvin et al., 1987). The 1-Ma olivine basalt fills topography, appears not to be faulted, and is virtually flat (Fig. 3.19). Northwest of highway (on left), Gila beds locally dip 5-10° toward the San Francisco Mountains fault zone, which parallels highway about 2.5 mi away. Volcaniclastics of Spears Group and andesite of Dry Leggett Canyon crop out in low hills west of fault zone. **3.0**

53.2 MP 16. Passing through settlement of Cruzville. Roadcut on right, at curve, is Gila Formation overlying Miocene olivine basalt, which is exposed on the back side of the cut. Continue on NM-12 with excellent views of Apache Creek water gap ahead (Fig. 3-20), where Tularosa River has cut through basalt flow dated at 0.9-1.0 Ma by conventional K-Ar whole rock method (Bikerman, 1972; Marvin et al., 1987). Downcutting by Tularosa River thus represents at least 330 ft of erosion since eruption of the basalt flow at Apache Creek. More precise Ar/Ar dating of the basalt may indicate a longer time for this amount of erosion. Older basalt flows, exposed at river level in this area, have Miocene K-Ar ages of about 13 Ma (Marvin et al., 1987), and an Ar/Ar age by Bove of 7 Ma. **1.0**

54.2 MP 17. 1-Ma basalt flow caps ridge to right. **2.0**

56.2 MP 19. Cross bridge over Apache Creek; this crossing was not always so easy (Fig. 3.21) Now in western part of Squirrel Springs Canyon quadrangle (Rhodes and Smith, 1976, fig. 2). **0.1**

56.3 Apache Creek store and junction with NM-32 on left. **Turn left onto NM-32**. Gila beds beneath flat-lying Apache Creek basalt flow strike about N35°E and dip about 10° northwest in roadcut on right (Fig. 3.22). Petroglyphs in basalt flow at top of mesa across from Apache Creek Store. See following minipaper by Wells. **2.0**

APACHE CREEK ARCHAEOLOGY

Stermon Wells

New Mexico State Parks, Santa Fe, NM 87504

Prehistoric village sites in the Apache Creek and Tularosa River drainages were cataloged and sketched by Walter Hough in 1907. In those days walls were still standing on some of the terraces and hills beside the streams. Some of these ruins may be about a thousand years old.

Along NM-12 and NM-32 today, most early village sites are hard to see and may only be noticed by traces of ground disturbance or recent digging. Where once stood multi-level apartment houses with hundreds of small cell-like rooms and adjoining underground kiva chambers now only piles of rocks with a sprinkling of small ceramic shards remains. Not a single Tularosa Phase (1100-1200 AD) ruin has been preserved or restored. No road sign indicates these sites along the way, or speaks of these old people at all. Generations of treasure hunters and archaeologists have combed these ruins, and carried all their specimens elsewhere.

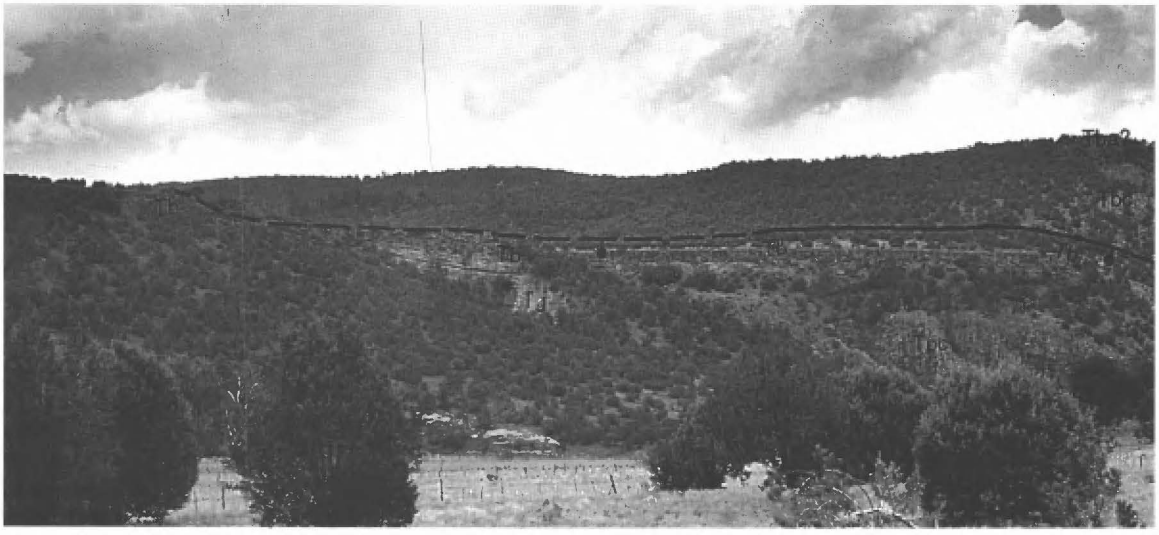

FIGURE 3.19. View east from NM-12 near Cruzville showing basalt of Apache Creek (~ 1 Ma), Tb, unconformably on gently tilted beds of the Gila Formation, Tg. Tbc, Bloodgood Canyon Tuff; Tba, Bearwallow Mountain Andesite. Basalt of Apache Creek was probably deposited against older fault scarp, a buttress unconformity?

The basalt bluffs above the Apache Creek store have an interesting collection of petroglyphs pecked into them, and it is a worthwhile climb to see them. Many designs may pertain to Pueblo religion, as well as a very nice looking buffalo!

From the top of this mesa you probably would have been able to see more buildings in 1200 AD than you can see today. Farming may have been more intensive also, even though it was all done by hand. Paul Sidney Martin (1959), of the Chicago Natural History Museum and a leading authority on the local archaeology, found much evidence of agriculture in these valleys. He excavated Tularosa Cave, about 10 mi to the northeast, up the Tularosa River, and discovered that several different kinds of corn, kidney and tepary beans, two kinds of squashes, as well as bottle gourds were being grown in these fields.

Martin and his associates wrote numerous papers and books describing their findings in this area. Their work shed significant light on the antiquity of maize agriculture in the Southwest. Corn may have been introduced as early as 2500 BC, and by perhaps 200 AD the local inhabitants had become quite dependent on it as a staple crop (Martin, 1959). Evidently by 1200 AD people in these valleys had become excellent farmers, as well as being remarkable experts in craft arts such as weaving, pottery and basketry. Local residents also hunted and foraged a wide variety of wild animals and plants to complement their agricultural products.

From the hill overlooking the Apache Creek store, the geography of these stream valleys suggest that they might be excellent natural trail routes, as they were. The modern highways still follow the old trails and arrive at the most significant ancient ruins (or go through them). The distribution of larger ruins along stream drainages throughout southwestern New Mexico in many cases defines the old trail networks. Most of these large ruins were less than a day's walk apart from each other along the natural watercourses, resulting in a very different settlement and land use pattern than occurs today. It allowed people to make maximum use of the arable land and available water resources with the level of technology they had at that time. Trails to the next town stopped at all the farms along the way, thus maintaining a web of trade and social network among the people.

Cross-finds of pottery have shown that people were in trade contact from Chaco Canyon to the Mimbres country. Although the extent and frequency of these contacts is unknown, geography dictates that Apache Creek was on one of the most important trails between the two areas.

About 3 mi up Apache Creek stand the ruins of a stone pueblo containing pottery and remains datable to 1000-1200 AD and related to the Tularosa culture. This pueblo directly overlies the pithouses of an earlier period from 800-900 AD, having pottery and architecture identical with that being used at the same time in the Mimbres region, over 150 mi to the south. This similarity strongly suggests common roots in the pithouse period for these two later groups and lends credence to the idea of a "Mogollon Culture" in these mountains. There has always been much academic discussion of whether these people were more "Mogollon" or "Anasazi", since they were influenced a great deal by both groups.

During the rise of the Chaco civilization, black on white pottery styles became prevalent throughout the entire region, and Tularosa pottery is one "Anasazi" style that has been found in many parts of the San Juan basin. Chacoan "roads" may be traced as far south as Zuni Salt Lake, about 50 mi north of Apache Creek, and trails run south from there through the mountain passes.

The inhabitants of the Apache Creek area employed Chacoan ideas of masonry in their wall construction, but were less adept in their efforts. Ruins 50 to 60 mi north of Apache Creek were more obviously part of the Chaco network in terms of architecture and artifacts. This area may well represent a prehistoric border of some kind between larger cultural groups, with a consequent mixing of cultural traits.

Oddly enough, there has been hardly any recognizable evidence in the archaeological record for contact between the Tularosa region and the Rio Grande. And even though Apache Creek was named for the Apache tribe, there is little recognizable evidence that they were here either. Around the Apache Creek store the map shows canyons named First, Second and Third Apache Canyons. There is an Apache Mountain nearby. Obviously the Apache figure importantly in the long

FIGURE 3.20. Apache Creek water gap is at the confluence of Apache Creek and the Tularosa River. The 1 Ma basalt flow which caps the mesas on opposite sides of the gap probably flowed down an ancestral Apache Creek, to the left of the photograph, into the Tularosa River valley, where the Tularosa eventually cut through the flow into the underlying Gila Formation to form the water gap.

FIGURE 3.21. Pat Birmingham (horseback) and Ambrocio Carrejo crossing Apache Creek in 1929. Courtesy of Buz and Beverly Easterling, Quemado Lake Estates.

FIGURE 3.22. View northward up Apache Creek and NM-32 across the San Francisco Mountains fault zone (SFZ) where it turns nearly east-west near the northeast end of the Reserve graben. Rocks north and west of the fault zone are andesite of Dry Leggett Canyon and younger units of the Spears and Mogollon groups as in Apache Mountain and Tularosa Mountain.

history of this area. In terms of the archaeological record, it is surprising that the 400-year tenure of the Apache left so little evidence of occupation, compared to the Tularosa people who left their subtle, but definite, mark on this beautiful land.

A good collection of local artifacts may be seen at the Western New Mexico University Museum in Silver City. The library at New Mexico State University in Las Cruces contains copies of most of the archaeological reports published about the area.

58.3 MP 2. Approximate west edge of Squirrel Springs Canyon quadrangle; return into Cruzville quadrangle at ranch road just ahead on left. **1.0**

59.3 MP 3. Ranch road and cattleguard on right. Now crossing approximate trace of San Francisco Mountains fault zone, as we move from the edge of the Cruzville quadrangle into the Queens Head quadrangle, and from Gila Formation volcaniclastic rocks on the southeast side of the fault zone into Spears Group volcaniclastic rocks in the footwall on northwest side. Here is about where the San Francisco Mountains fault zone bends from a northeast trend to nearly east-west.

Although there are several hundred feet of throw on the San Francisco Mountains fault zone, the Quaternary basalt flow of Apache Creek continues to crop out in patches along the ridge crest on the east side of Apache Creek with little or no discernible offset (T.L.Finnell, unpubl., 1987). This flow must have entered the ancestral Tularosa River valley essentially at grade along an ancestral Apache Creek drainage from a source area farther northwest. **0.4**

59.7 Outcrops of Spears Group include white sandstone beds and brown conglomerate beds that contain boulders of fossiliferous Paleozoic limestone and Precambrian crystalline rocks. **0.6**

60.3 MP 4. Andesite of Dry Leggett Canyon caps ridge on left, above beds of lower part of the Spears Group. **0.7**

61.0 Approaching curve to left; cliff-forming unit in slopes ahead on right is 15-30-ft-thick tuff of Bishop Peak (34.7 Ma), interlayered with Spears Group volcaniclastics and overlain by andesite of Dry Leggett Canyon. **1.3**

62.3 MP 6. New Mexico Ranch for the Deaf on left at mouth of Lee Russel Gulch. Good collecting up this gulch for Luna blue agate within andesite of Dry Leggett Canyon. **2.0**

64.3 MP 8. Mouth of Whiskey Canyon. Old NM-32, as shown on 1965 Queens Head topographic quadrangle map, goes up Whiskey Canyon. Stay left on new alignment of NM-32. Roadcuts ahead, mainly on east side of road, consist of Spears Group volcaniclastic sedimentary rocks beneath the andesite of Dry Leggett Canyon. The volcaniclastic rocks include a lower, white, pumice-bearing sandstone sequence and an upper, green sandstone sequence. Both sequences locally contain distinctive, thin, centimeter-scale, pink, plagioclase-bearing tuff beds that apparently are juvenile and/or reworked ash layers. The ash layers probably represent premonitory eruptions associated with the source of the overlying lava flows of Dry Leggett Canyon. Plagioclase was collected for dating from several of the ash layers in the belief that it was sanidine, but only a couple of sanidine crystals were recovered from several age samples, and the plagioclase has given erratic Ar/Ar ages.

About 1 mi above the mouth of Whiskey Creek, Apache Creek branches into Hardcastle Canyon on the left and Deep Canyon on the right. NM-32 follows Deep Canyon (Fig. 3.23). Near the junction of the

FIGURE 3.23. Oblique aerial view overlooking Hardcastle Canyon and Stop 2 in Deep Canyon. Ts, Eocene-Oligocene Spears Group; Tla, Andesite of Dry Leggett Canyon.

FIGURE 3.24. Roadcut along NM-32 shows green and white sandstone in lower Spears Group, overlain by columnar jointed andesite of Dry Leggett Canyon at right side of photograph.

FIGURE 3.26. Partly welded surge beds with black fiamme beneath geology pick.

canyons, and in the spectacular roadcuts ahead, on the left, in Deep Canyon, the green sandstone intertongues with the white sandstone.

Drive through roadcut with green, bedded sandstone to left (Fig. 3.24), to where the overlying andesite lava flows of Dry Leggett Canyon come down to road level. We will try to park everyone in the wide pull-out on the west (left) side of the road; **prepare to make a U-turn into the parking area** so that we will be headed correctly to return to Apache Creek store and NM-12, when we leave Stop 2. **1.7**

66.0 **STOP 2. Make U-turn into parking area on west side of road**. At this stop, we shall focus on the pink beds between lava flows of the andesite of Dry Leggett Canyon at the parking area (Fig. 3.25), and the green, volcaniclastic sandstone sequence and interlayered pink ash beds down the road beneath the lava flows (Fig. 3.24).

Here above the parking area, what initially appears to be a thin sedimentary interval between lava flows is complicated by the presence of dark layers (Fig. 3.26) having lenses of perlitic glass as much as several centimeters long (Figs. 3.27, 3.28). These appear to be fiamme, i.e. collapsed or fused pumice fragments (Fig. 3.29), which implies a volcanic rather than a fluviatile sedimentary origin for these beds. The presence of fine-grained, graded and crossbedded sedimentary layers and dune forms mixed with the pyroclasts (Figs. 3.30, 3.31) rules out a simple pyroclastic flow origin. However, at least one ignimbrite (tuff of Bishop Peak) is interlayered in the sandstone sequence more or less immediately beneath the andesite of Dry Leggett Canyon, in the lower part of Apache Creek canyon. That the bedded interval near the base of the andesite flows at this Stop might be the tuff of Bishop Peak was considered, but the latter is characterized by sanidine and biotite, and minor clinopyroxene phenocrysts rather than by the plagioclase, clinopyroxene and orthopyroxene phenocrysts that dominate the phenocryst assemblage in the beds here.

Our collective, but tentative, conclusion is that the various volcanic and sedimentary features exhibited here represent some type of pyroclastic surge deposit

FIGURE 3.25. Pink, partly welded, pyroclastic surge deposits between andesite lava flows of Dry Leggett Canyon along NM-32 in Deep Canyon.

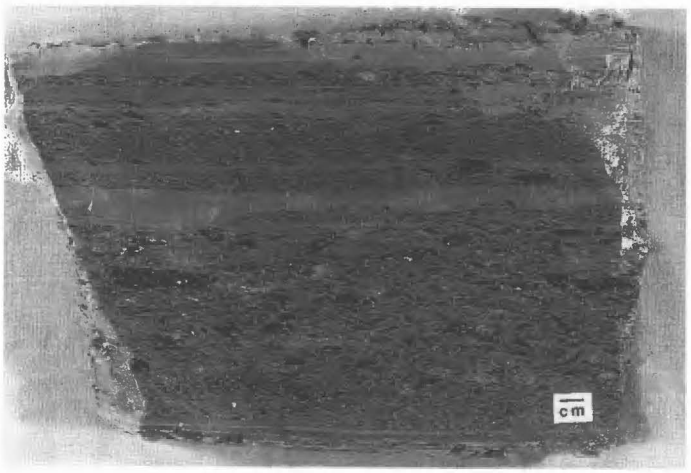

FIGURE 3.27. Polished slab of welded surge showing centimeter-scale, welded glass lenses (fiamme).

FIGURE 3.28. Photomicrograph, in plane polarized light, of an entire thin section (~ 3.5 x 2 cm.) of welded pyroclastic surge materials showing perlitic glass lenses (fiamme), p; fine, graded ash, a; and plagioclase and pyroxene phenocrysts. See Figs. 3.29 and 3.31 for closeup views of areas in lower and upper rectangles, respectively.

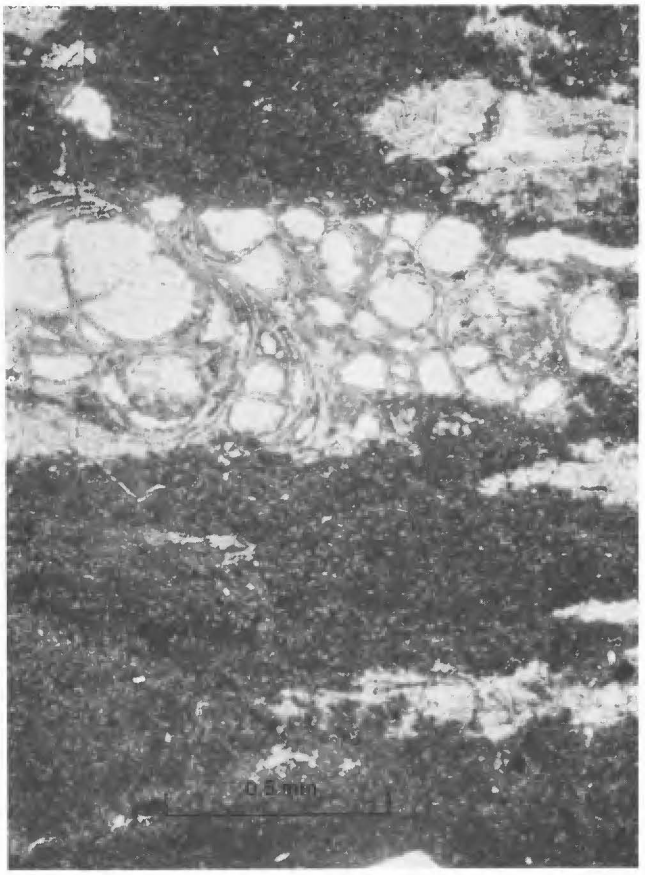

FIGURE 3.29. Welded glass lens (fiamme) with peritic hydration cracks surrounded mainly by fine ash.

that originated in conjunction with the eruption of the andesite lava flows with which the bedded deposits are intercalated.

Pyroclastic surge deposits have been divided into three types: base surge, ground surge and ash-cloud surge (Fisher and Schmincke, 1984; Cas and Wright, 1987), but it is not perfectly clear which type is present here. All three types of surge deposits are related in one way or another to the eruption columns associated with pyroclastic flows, or to processes related to the pyroclastic flows themselves. However, Cas and Wright (1987, p. 120) cited evidence of pyroclastic surge deposits, which they call ground surge, produced by eruption column collapse associated with *fallout* deposits that were *not* accompanied by pyroclastic flows. No discrete pyroclastic flow or ignimbrite is present here, and thus the bedded interval may comprise a pyroclastic surge deposit associated with fall deposits related to the eruption of andesite flows of Dry Leggett Canyon. If so, in order to maintain heat sufficient for welding to occur, the surge must have been deposited while the underlying flow was still hot and then covered almost immediately by the overlying flow.

The presence of small-scale dunes and antidunes supports the surge hypothesis, and the phenocrysts present in the glassy fiamme, mainly plagioclase and pyroxene, suggests comparable chemical compositions for the

FIGURE 3.30. Dune structure in pyroclastic surge beds at Stop 2.

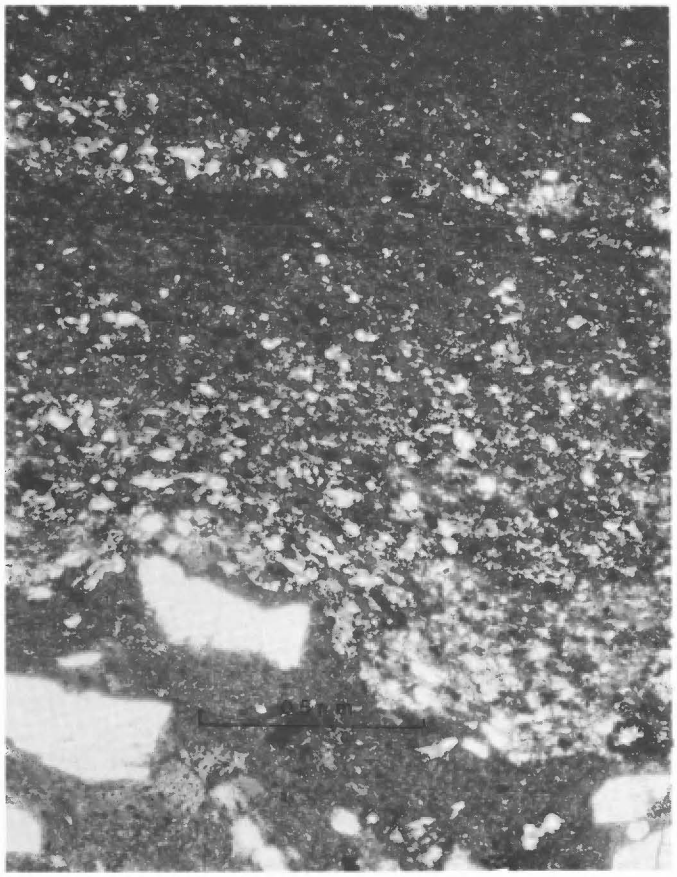

FIGURE 3.31. Photomicrograph showing normally graded ash layers in pyroclastic surge beds at Stop 2.

flows and the bedded surge. However, chemical analyses of the underlying flow and a glassy lens show about 7.0% more silica in the perlitic glass than in the flow (Table 3.2). The chemistry of the glass seems to indicate different sources for the andesite flows and the fiamme, but turbulent flow processes during deposition of the pyroclastic surge could have rendered the glass analyses essentially meaningless, and thus the flows and surge deposits may still be chemically related.

TABLE 3.2. Chemical analyses of andesite of Dry Leggett Canyon and glassy clots (fiamme) from pyroclastic surge beds between Dry Leggett Canyon andesite flows at Stop 2. X-ray spectrography; laboratory chief, J.S. Mee; analysts, D.F. Siems and J.S. Mee.

	glassy clots	porphyritic andesite
SiO_2*	60.2 (64.2)	56.0 (57.2)
Al_2O_3	15.9	16.2
$FeTO_3$	4.26	8.03
MgO	3.13	4.08
CaO	4.12	6.78
Na_2O	3.14	3.29
K_2O	2.06	2.28
TiO_2	0.71	0.99
P_2O_5	0.21	0.23
MnO	0.08	0.11
LOI (925°C)	5.51	1.52
SUM	99.32	99.51

*SiO_2 values in parentheses are normalized volatile free.

Ground surge deposits are generally found within a few miles of their source, indicating that Stop 2 is near a vent for the andesite of Dry Leggett Canyon. Similar surge(?) deposits are present on the northeast flanks of Prairie Point Peak, north of Dry Leggett Canyon, which suggests another possible source for the Dry Leggett flows.

Keep these deposits in mind when we examine pyroclastic surge beds of probable ash-cloud origin at Stop 3. Walk back along the highway to the thick sandstone sequence, where you will find sedimentary structures and other features pertinent to the interpretation of the origin and provenance of these deposits. Keep your eyes and ears open for rock falls from these cliffs; the concrete barriers along the edge of the road are not without an obvious purpose. If you brought a hard hat, it might not be a bad idea to wear it.

The white and green sandstone beds in the Spears Group are at least 800 ft thick in this area; the base is not exposed. Sedimentary structures, such as massive to thin bedding sequences of well-sorted sandstone and silt, fine-grained concentrations of heavy minerals (Fig. 3.32), and shallow channels (Fig. 3.33), are interpreted as overbank deposits on a broad alluvial floodplain. The volcaniclastic origin of these fluvial deposits is well documented by the presence of sand-sized and larger clasts of white to gray pumice throughout most of the sequence, but particularly in the white sandstone. Even more conspicuous are the multiple pink beds, from less than 0.5 in. to greater than 7.5 in. thick, of very fine-grained to medium-grained, (reworked?) ash containing pumice and plagioclase and biotite crystals. These ash beds have phenocryst assemblages more like those of the overlying lava flows than like the tuff of Bishop Peak, which also occurs near the base of the Dry Leggett Canyon flows in the lower part of the canyon of Apache Creek. The tuff of Bishop Peak seems to be absent in this immediate vicinity, either having pinched out or having been eroded before the andesite flows were erupted. Argon 40/39 ages for biotite from some of the ash layers could provide information about the minimum age of the sediments beneath each of the dated ash layers.

Chamberlin and Harris (this volume) describe a correlative interval of pumiceous sandstones, the volcaniclastic unit of Cañon de Leon, exposed on the north flank of Escondido Mountain, 23 mi to the northeast. Sanidine ages of pumice clasts indicate that these beds range from 35.33 ± 0.06 Ma at the base to 34.17 ± 0.13 Ma at the top of this unit, which is about 600 ft thick. This age range includes the tuff of Bishop Peak and the andesite of Dry Leggett Canyon (McIntosh and Chamberlin, this volume).

Return to cars and retrace route to junction of NM-32 and NM-12. 9.4

75.4 Junction, NM-32 and -12. **Turn left onto NM-12** and drive northeast through the Tularosa River water gap, where the Gila Formation is capped by the 1-Ma Apache Creek basalt flow on both sides of the highway. We are now back in Squirrel Springs Canyon quadrangle. **0.7**

FIGURE 3.32. Green sandstone beds in lower Spears Group at Stop 2 showing streaks of heavy minerals. Sandstone beds are separated by pink, shaly and pumiceous layers, interpreted to be reworked? volcanic ash. Pencil is about 5.5 in. long.

FIGURE 3.33. Channel(?) in green and white sandstone in lower Spears Group at Stop 2. Left side of channel appears to be a slip surface.

76.1 Ranch road on right. To left, Gila Formation is capped by the 1-Ma basalt flow at Apache Creek, but on right at river level, beside the various colored pick-up truck beds being used as cattle feeders, and in roadcut just ahead, more young (Miocene) basalt, in lower part of Gila Formation, has been dated at 7.0 ± 0.4 Ma by whole rock Ar 40/39 by D.J. Bove. **0.2**

76.3 MP 20. Ahead, north of the highway, the San Francisco Mountains fault zone swings across our view and trends nearly east-west as the Reserve graben is squeezed down to its apparent termination near the head of the Tularosa River valley. **4.0**

80.3 MP 24. Approximate north edge of the Squirrel Springs Canyon quadrangle; entering Aragon quadrangle (T. L. Finnell, unpubl., 1989). Outcrops in roadcuts, and on both sides of the highway, are Gila Formation within the narrowing Reserve graben. As the highway and the valley swing to a more nearly east-west trend, the San Francisco Mountains fault zone is only about 1300 ft or less north of, and parallel to, the highway. **1.0**

81.3 MP 25. Road on left. San Francisco Mountains fault zone north of here includes a fault about 1300 ft north of the highway that is down to the south, and a parallel, vertical fault about 0.6 mi north of highway that is down to the north. Spears Group volcaniclastic rocks crop out in a narrow horst between faulted Gila beds on both sides. Richard Chamberlin found both sub-horizontal and dip-slip (near vertical) slickensides in gouge along this nearly vertical fault, indicating a complex history of movement for this fault zone. **1.0**

82.3 MP 26. Santo Nino Catholic Church in Aragon on left. San Francisco Mountains fault zone is about 650 ft behind the church. A 15- to 30-ft-thick ignimbrite beneath the andesite flows of Dry Leggett Canyon in the footwall of the fault zone appears to be Kneeling Nun Tuff with a 40/39 Ar age of 34.8 ± 0.54 Ma. Aragon is named for a family that arrived in New Mexico in 1693 (Pearce, 1965). **0.8**

83.1 Cross San Francisco Mountains fault zone. Here at the north end of the Tularosa Mountains, off to the east and south (right), the Reserve graben is en echelon with the San Agustin graben, the south end of which is about 10 mi to the southeast. Thus, the Reserve graben seems to be terminated on the north by a zone of east-west-trending faults, and major extension is shifted to the San Agustin graben. On the other hand, the north-northeast fault trend continues into the Quemado area to the north with the Hickman and associated faults. A small trap-door like graben, the Sand Flat graben, (Fig. 3.4) appears to represent the eastward continuation of the Reserve and Luna grabens depression that links with the southwest end of the San Agustin depression near Horse Springs. See following road log entries. **0.2**

83.3 MP 27. Andesite of Dry Leggett Canyon crops out on both sides of the highway. Flows are within a horst that marks the San Francisco Mountains fault zone. Around curve to left, and straight ahead in lower slopes of Tularosa Mountain, on the north side of the highway, is the Tularosa Cave archeological site (Fig. 3.34; see minipaper by Wells, this roadlog). The caves are excavated in crossbedded, brown sandstone that normally underlies Squirrel Springs Canyon Andesite, but here the sandstone is overlain unconformably by coarse debris flows of unknown age within the Gila Formation. The debris flows, which contain blocks of Bloodgood Canyon Tuff, Squirrel Springs Canyon Andesite, and other clasts of local origin, as much as 10 ft long, are graded almost to the level of the present drainage, which suggests that the debris flows could be approximately as young as the 1 Ma basalt flow at Apache Creek. However, the apparent induration of the debris flows indicates that they may be much older.

The rocks in the upper part of Tularosa Mountain consist of volcaniclastic sandstone overlain by a volcanic sequence that includes Vicks Peak Tuff, Squirrel Springs Canyon Andesite, Shelley Peak Tuff, Bloodgood Canyon Tuff, and Bearwallow Mountain Andesite. **1.0**

84.3 MP 28. Up side canyon to right, about 0.5 mi, in Tularosa Canyon quadrangle (Ratté, 1992), Bearwallow Mountain Andesite contains abundant, small, upper(?) crustal xenoliths, a few centimeters

FIGURE 3.34. Tularosa Cave archeological site west of NM-12 at about MP 27 east of Aragon, New Mexico. Caves are in brown, crossbedded sandstone in upper part of Spears Group at unconformable contact with overlying debris deposits in Gila Formation, which contains 3-6-ft-wide clasts of Bloodgood Canyon Tuff and Squirrel Springs Canyon Andesite and other older rocks (see minipaper by Wells, this road log.).

across, that include gabbroic and granitic rock types, gneissic hornblende diorite?, and pyroxenite.

Around the curve ahead on left, crossbedded, brown sandstone in roadcut underlies landslide deposits coming off Tularosa Mountain. Across the Tularosa River on the right, the same brown sandstone underlies thin Squirrel Springs Canyon Andesite and Bloodgood Canyon Tuff, overlain by Bearwallow Mountain Andesite. Patchy outcrops of Gila Formation on the ridge top, above the Bearwallow Mountain Andesite, were prospected for uranium by means of bulldozer cuts in the 1960s. This accounts for the prospects shown on the Tularosa Canyon and Aragon quadrangles, according to U.S. Forest Service officials at Reserve. **1.0**

85.3 MP 29. Between the mobile home on the right near Tularosa Spring, and MP 29, we crossed a fault that is one of several approximately east-west-trending faults on the northeast side of Tularosa Mountain that drops the section down to the north. In combination with the arcuate, down-to-the-east Cañon del Buey fault (see First Day road log) these down-to-north faults form the Sand Flat graben. The reversals in fault block asymmetry from the Reserve graben (down to southeast) to down to northwest in the Sand Flat graben is apparently facilitated by a north-trending, arcuate accommodation zone on the east flank of Apache Mountain. The east end of the Sand Flat graben rises to form a ramp against the south end of the Hickman fault zone. **0.6**

85.9 Sand Flat Road on left. Note buff-colored Gila Formation cropping out in grass above road junction, at eastern edge of Aragon quadrangle. **0.2**

86.1 Highway bridge across Cañon del Buey in Tularosa Canyon quadrangle. The andesite lava flows exposed in Cañon del Buey are correlated with the Bearwallow Mountain Andesite, although they contain hornblende, biotite and bright green pyroxene phenocrysts, not usually present in the Bearwallow Mountain Andesite. However, they have chemical compositions similar to Bearwallow Mountain Andesite flows on the lower slopes of Mangas Mountain in the northern part of the Tularosa Mountain quadrangle. **0.2**

86.3 MP 30. Highway approximately follows the contact between Gila Formation and the underlying Bearwallow Mountain Andesite flows. The Gila Formation in this part of the Tularosa River valley is essentially a clastic wedge on the south-facing dip slope of the small Sand Flat half graben (Fig. 3.4). The footwall of this half graben lies 2.5 mi south of the highway, where Spears Group volcaniclastic sedimentary rocks are uplifted along more or less east-west faults between the highway and the lower slopes of Wagontongue Mountain, at the south edge of the Tularosa Canyon quadrangle. Wagontongue Mountain is the main ridge on the skyline south of the highway; the ridge crest is in the John Kerr Peak quadrangle, which has not been mapped in detail, but is the site of the John Kerr Peak dacite dome complex (Smith, 1976; Smith et al., 1976), about 12-14 Ma (Marvin et al., 1987). **2.8**

89.1 Junction on right. A combination of ranch roads and forest trails will take one close to the unique locality where the Bearwallow Mountain flows contain small centimeter-size crustal xenoliths, including granitic, gabbroic, quartz dioritic and pyroxenitic types of inclusions. The xenolith-bearing rocks are in the creek bed in a small box canyon, on the downstream side of a tight horseshoe loop, near the north edge of sec. 10, T5S, R16W, about 0.5 mi from the west edge of the Tularosa Canyon quadrangle. This locality can also be reached from the mouth of the canyon, in the Aragon quadrangle, in the northwest corner, sec. 10, as earlier described at 84.3 miles (MP 28) in this road log. **0.2**

89.3 MP 33. Bloodgood Canyon Tuff underlies Gila Formation in roadcuts from here to the Continental Divide. **1.6**

90.9 Continental Divide, elevation 7312 ft. **1.4**

92.3 MP 36. About 16 ft of Shelley Peak Tuff (28 Ma), from a source in the Mogollon Mountains, is sandwiched between Squirrel Springs Canyon Andesite, below, and Bloodgood Canyon Tuff above, in low ridges on both sides of highway between here and east edge of Tularosa Canyon quadrangle. **1.5**

93.8 East edge of Tularosa Canyon quadrangle. Entering Bell Peak quadrangle (Ratté, unpubl. 1986-1987). Hills projecting above alluvium and colluvium on both sides of highway are Squirrel Springs Canyon Andesite overlain by Shelley Peak and Bloodgood Canyon Tuffs and Bearwallow Mountain Andesite. **0.5**

94.3 MP 38. Views on right (about 12:00 to 3:00) of southwest part of Plains of San Agustin (San Agustin graben). **2.0**

96.3 MP 40. Junction; north end of Bursum Road on right just south of milepost. Highway is on older alluvial fans that are dissected by the present Patterson Canyon

FIGURE 3.35. View northeast along NM-12 to Cerro Caballo near vent outcrops of the Horse Springs dacite (Ratté et al., this volume). Horse Mountain is on skyline to left.

drainage. Mangas Mountains north of highway (on left) are mainly Bearwallow Mountain Andesite. **2.0**

98.3 MP 42. Views of Horse Mountain on skyline at about 11:00, and Cerro Caballo (Stop 3) straight down road (Fig. 3.35). Cross main Patterson Canyon, just ahead; Rincon Canyon road is on left between Patterson Canyon and Rincon Canyon. Bloodgood Canyon Tuff is overlain by Bearwallow Mountain Andesite on nose of ridge on east side of Rincon Canyon, less than 0.3 mi north of highway; low hills behind that ridge are capped by Miocene(?) "big feldspar" basalt, which overlies Squirrel Springs Canyon Andesite, which overlies rhyolite lava flows of Bat Cave Wells on both sides of the highway. The rhyolite flows were called Rhyolite of Wye Hill by Bornhorst (1976), but Wye Hill is not identified on modern maps, so flows are now named for tentatively correlative outcrops along south side of Plains of San Agustin at Bat Cave Wells. **2.0**

100.3 MP 44. Ranch road on left. A pull-off just ahead on right is a good place to park to examine outcrops of the Horse Springs dacite along the north side of the highway for about the next half mile. Along the right side of the highway, the outcrops are of Eocene tuffs (Blue Canyon, Rock House Canyon), which underlie the Horse Springs pumiceous dacite cropping out farther south of the road in the cavernous, columnar jointed cliffs. Stop 3 is on the back side of this ridge, where the exposures are somewhat more informative. However, float of the jasperoid and quartz monzonite inclusions to be seen in the dacite at Stop 3 can also be found here along the north side of the highway. **1.0**

101.3 MP 45. East edge of Bell Peak quadrangle. Enter Horse Mountain West quadrangle (Ratté et al., 1991). Blue Canyon Tuff in roadcut on north side of highway. Here this phenocryst-rich tuff shows a sharp change from densely welded to poorly welded material. There is no known source for this apparent regional ash-flow tuff. A $^{40}Ar/^{39}Ar$ analysis for a sample from this outcrop indicates an age of 33.7 Ma (McIntosh et al., 1991). **0.5**

101.8 **STOP 3. Turn right at ranch road**; there may be a steel cable across cattleguard; the cable may be locked. We are able to enter here through the courtesy of Dave and Karin Farr. Follow lead car to parking area about 2 mi from cattleguard at highway. Outcrops in low ledges along route are mainly ash-flow tuffs of the upper part of the Datil Group, mostly Rock House Canyon and Blue Canyon Tuffs, 34.4 and 33.7 Ma, respectively.

The primary purpose at this Stop is to examine the Horse Springs dacite in the outcrops on the east-facing slopes of Cerro Caballo, an informal name for the ridge west of us. To the east are the San Agustin plains, a.k.a. the San Agustin basin and the San Agustin graben, and the site of prehistoric (Quaternary) lake San Agustin and its numerous abandoned shorelines. Across the plains is a line of 25-Ma Bearwallow Mountain Andesite volcanoes, including Luera Peak, Pelona Mountain and O Bar O Mountain. On a clear day, one can see Tres Montosa peaks over by the Very Large Array (VLA), the National Radio Astronomy Laboratories site at the east end of the Plains of San Agustin. The mid-Miocene, dacitic Horse Mountain volcano is at the north edge of the plains, and at the base of Horse Mountain, a 0.6-mi-long hogback of Permian sedimentary rocks is believed to be a remnant of the Laramide Morenci uplift (Cather and Johnson, 1984; Chamberlin and Anderson, 1989), and the location of the Mogollon Rim in this area. The low hills south of NM-12, at New Horse Springs, contain the most complete sequence of upper Datil Group ignimbrites and interlayered Spears Group volcaniclastic rocks in this area. The site of the first of several wells drilled during recent petroleum exploration in this region is just west of the lava flows on the west ridge of Horse Mountain, beside the road to Dutch Oven Pass, several miles north of here.

The Horse Springs dacite is largely a proximal pyroclastic vent deposit, which here consists of a lower sequence of pyroclastic pumice flows, capped by discontinuous remnants of ash-cloud surge beds, and overlain by a thick block-and-ash deposit (Fig. 3.36). The lower pumice flows contain pumiceous dacite blocks, which show reverse size grading particularly near the top of the two upper flows, which we will traverse. The surge beds are present at the base of the cliffs. The cliffs also exhibit ancient fumarole tubes, or elutriation pipes, at the base of the block-and-ash flows, which is unusual in that such features are usually at the top of flow units.

Both the pumice flows and the block-and-ash flows contain cognate, porphyritic quartz monzonite inclusions. These are generally lapilli size or smaller in the

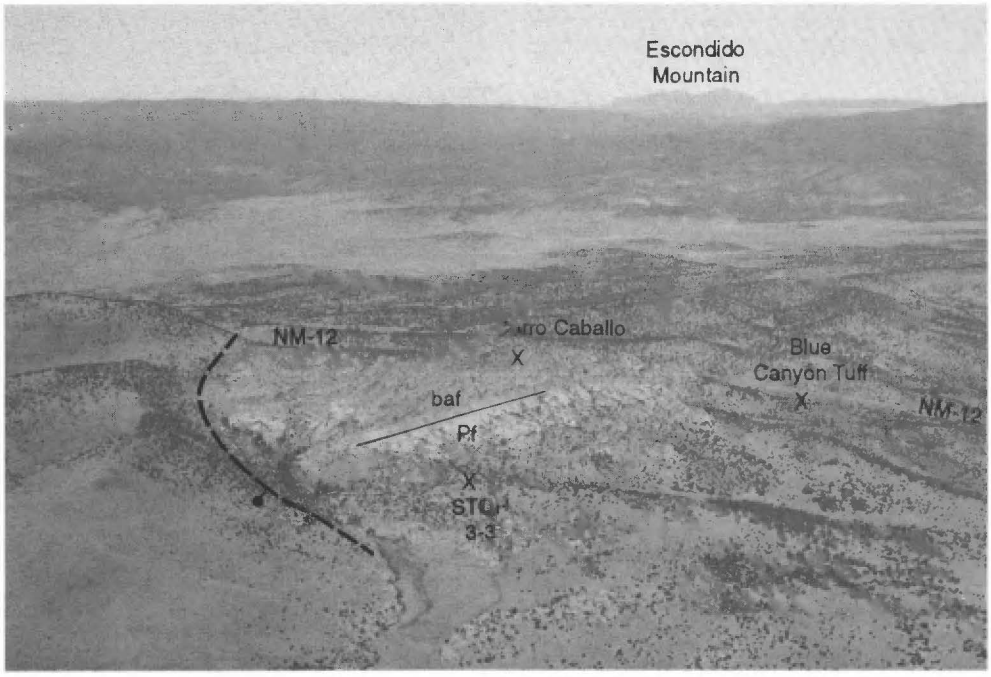

FIGURE 3.36. Aerial photograph looking northwest across Cerro Caballo showing location of Stop 3 and contact between pumice flows, pf, and overlying block-and-ash-flows, baf, of Horse Springs dacite.

pumice flows, but attain dimensions of 6-10 ft in the block-and-ash flows, as do the juvenile pumiceous dacite blocks. The block-and-ash flows also contain accidental inclusions of Paleozoic sedimentary basement rocks, which apparently represent the same sedimentary sequence that crops out in a 0.6-mi-long hogback about 6 mi away at the base of Horse Mountain. The accidental inclusions are largely jasperoidized (silicified) blocks of limestone, calcareous argillite and quartzite from the Lower Permian Yeso Formation, Glorieta Sandstone and San Andres Limestone. These inclusions also are mineralized (iron and zinc), and where in place, many are enclosed in skarn-like reaction rims; "skarn-like" because the reaction rims contain clay minerals as well as calc- silicate minerals, which are dominantly diopside and minor garnet. Our present interpretation of the dacite deposit and its inclusions is described in more detail in the article on the Horse Springs dacite (Ratté et al., this volume), but is summarized here as follows:

1. A shallow body of quartz monzonite magma initially rose into contact with, and probably stoped its way into, the Paleozoic sedimentary rocks, and jasperoidization and mineralization may have occurred at this time, while a crystalline hood of coarsely porphyritic quartz monzonite formed at the top of the magma (Ratté et al., this volume, fig. 20).

2. Confining pressure in the magma chamber was eventually relieved by fracturing in the crystallized hood, and pumice flows were deposited from an eruption column that entrained small fragments of the ruptured quartz monzonite hood. These eruptions ended with the ash-cloud surge deposits that settled atop the pumice flows.

3. The premonitory pumice flow eruptions were followed closely by a massive, paroxysmal block-and-ash eruption, which not only carried 6-10 ft blocks of pumiceous dacite, but also equally large blocks of cognate porphyritic quartz monzonite. In addition, the block-and-ash flows entrained accidental inclusions of the jasperoidized Paleozoic sedimentary rocks, which appear to be concentrated near the top of the greatest concentration of large pumiceous dacite and quartz monzonite blocks.

4. The skarn-like rims around the accidental calcareous inclusions must have been acquired after eruption and during cooling of the block-and-ash deposit, because it seems unlikely that the fragile encompassing rims of friable diopside crystals could have survived eruption if they had been formed adjacent to the magma prior to eruption. Furthermore, the clay minerals in the skarn-like rims probably were derived by alteration of the enclosing dacite rather than from the inclusions.

5. The venue for mineralization is somewhat less certain. Iron and zinc oxides, which characterize the mineralization, could have formed adjacent to the magma chamber in reduced forms such as magnetite, that were erupted as part of the jasperoid inclusions, and later oxidized to hematite, magnesioferrite and other minerals now found in the surface deposits. Alternatively, mineralization and jasperoidization, as well as the skarn-like rims could have formed in place within the cooling dacite.

The reasons for suggesting that jasperoidization and mineralization took place at depth rather than after eruption of the dacite are:

1. The apparent absence of *unaltered* (non-jasperoidal) accidental inclusions, which might be anticipated in cooler parts of the deposit, although it may be

that the inclusions were all entrained in the earliest phase of the block-and-ash eruption, as suggested by their apparent concentration in its lower part.

2. The lack of mineralization associated with the ancient fumaroles at the base of the block-and-ash flows.

3. The Paleozoic sedimentary rocks adjacent to the magma chamber might have been more susceptible to alteration and mineralization than inclusions of the same rocks in the erupted dacite because of higher temperature and more trapped volatiles at depth.

One consequence of ruling out alteration and mineralization having occurred next to the magma chamber is to lessen expectations for possible economic deposits at depth.

The Horse Springs dacite also has implications relative to the origin of some of the regional ignimbrites in the Datil Group in this area. New Ar/Ar ages for the dacite and its quartz monzonite inclusions of 33.8 ± 0.03 Ma, and 33.6 ± 0.06 Ma, respectively, indicate that it is indistinguishable in age from the immediately underlying Blue Canyon Tuff. The Horse Springs dacite and Blue Canyon Tuff are also largely indistinguisable in chemistry and phenocryst mineralogy.

A caldera buried beneath the San Agustin Plains is a possible source for both the Blue Canyon Tuff and the Horse Springs dacite. This is an alternative to the proposed subsidence of the ~ 25x30 mi Crosby Mountains depression in response to the eruption of the Horse Springs dacite (Elston, 1984, table 1; Bornhorst, 1976; Jones, 1980). See minipaper by Chamberlin in First Day road log for additional discussion of the "Crosby Mountains depression" as proposed by Elston, 1984.

Return to NM-12 and turn right; resume road log. In the trees north of the highway, opposite this ranch road, are two large springs, each about 150 ft across, for which Horse Springs was named. **0.5**

102.3 Settlement of Old Horse Springs. Horse Springs was the setting for one of Louis LaMour's western novels, called "Conagher," but use of the name is about as close as the locale comes to being recognizable in "Conagher", so maybe it was another Horse Springs that the author had in mind! **2.3**

104.6 New Horse Springs, site of now defunct Horse Springs store and gas station. Ridges south of highway here offer one of the most complete sections of the upper Datil Group ash-flow tuff outflow sequence. Ar/Ar dates and paleomagnetic data are available for most of the units in this section (McIntosh et al., 1991,1992; Ratté et al., 1991). Tuffs present include Datil Well Tuff, tuff of Farr Ranch, Kneeling Nun Tuff, tuff of Lebya Well, Rock House Canyon Tuff, and Blue Canyon Tuff, interlayered with Spears Group volcaniclastic sedimentary rocks.

Road on left goes to Dutch Oven Pass and Collinsville. The Shell Oil Co. exploration well (SWEPI State No. 1), is located on the slopes above the road on its west side, about 5 mi from NM-12. **3.8**

108.4 East edge of Horse Mountain West quadrangle. Entering Horse Mountain East quadrangle (J. C. Ratté, unpubl. 1990). Highway traverses shoreline deposits of prehistoric lake San Agustin (see Weber, and McFadden et al. minipapers in First Day road log). South of highway, shoreline deposits give way to playa and lake beds. A drill hole in the southwestern part of the playa penetrated 2000 ft of lacustrine silt, clay and alluvial gravel beneath the playa; Tertiary pollen appear at a depth of 920 ft. Paleoenvironmental analysis indicates that prehistoric lake San Agustin dried up about 5000 years ago (Markgraf et al., 1983). **0.9**

FIGURE 3.37. Outcrops of pre-Tertiary rocks at the foot of Horse Mountain north of NM-12 at about MP-53. Pre-Tertiary rocks include Permian Yeso, Glorieta and San Andres formations.

109.3 MP 53. **OPTIONAL STOP 4**. About 0.6 mi north of highway, pre-Tertiary rocks crop out in a ridge about 400 m long (Fig. 3.37). The rocks include the Lower Permian Yeso Formation, Glorieta Sandstone, and San Andres Limestone (see following minipaper by Lucas and Kues). The pre-Tertiary rocks are overlain by float of round, pebble conglomerate like that in the Baca Formation to Spears Group transition, but the nature of the contact of these rocks with the underlying pre-Tertiary rocks is uncertain. However, seismic data supports the interpretation of a Laramide high below the Permian rocks on the flanks of Horse Mountain. The pre-Tertiary rocks probably represent a relic of a Laramide structural high that is now faulted beneath the Plains of San Agustin. This interpretation is supported by seismic data (L. Garmezy, personal commun., 1994). **1.0**

PERMIAN STRATA AT HORSE MOUNTAIN

Spencer G. Lucas[1] and Barry S. Kues[2]

New Mexico Museum of Natural History and Science, 1801 Mountain Road NW, Albuquerque, NM 87104; Department of Earth & Planetary Sciences, University of New Mexico, Albuquerque, NM 87131-1116

Charles Stearns (1962; see also Foster, 1964, and Willard and Stearns, 1971) first noted and mapped Permian strata near Horse Mountain, and Kottlowski and Foster (in Stearns, 1962) described a stratigraphic section through these strata in sec. 20, T4S, R12W, assigning them to the Yeso, Glorieta and San Andres formations and to an overlying Triassic(?) sandstone. Megafossils collected from a gray limestone on the crest and back slope of a hogback south of Horse Mountain indicated, according to Rousseau Flower, the presence of the San Andres Formation there. Dane and Bachman (1965), on the geologic map of New Mexico, showed about 2 mi² of Permian strata to the south, overlain by Triassic rocks in the north. No further work on or mention in the literature of the Horse Mountain Paleozoic strata occurred until Lucas and Hayden (1989, p. 203, fig. 10) described and illustrated these units and concluded that no Triassic strata are present near Horse Mountain.

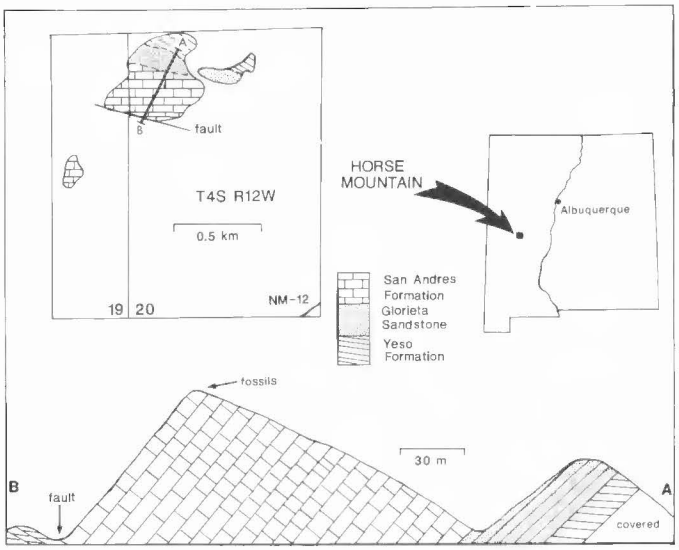

FIGURE 3.38. Geologic map and cross section of Permian strata south of Horse Mountain, Catron County, New Mexico.

Stearns' (1962, pl. 1) geologic map accurately depicts the distribution of Paleozoic strata south of Horse Mountain, which mainly crop out in the NW¼ sec. 20, T4S, R12W, with a small inlier in the SE¼ NE¼ sec. 19. In the larger outcrop area, the San Andres Formation forms a prominent, southeasterly dipping hogback; the stratigraphic section measured by Kottlowski and Foster in this area and our own observations lead to recognition of (in ascending order) the Permian Yeso, Glorieta and San Andres formations.

Kottlowski and Foster measured 61 m of faulted Yeso Formation, mostly gray and light red sandstones and thin limestone beds, with more than half of this thickness consisting of covered intervals. Our examination of the Yeso section began at the top of Kottlowski and Foster's section, where an oolitic dolomite about 10 m thick crops out. This dolomite is medium bluish gray (5B5/1) but weathers medium light gray (N6), moderate yellowish brown (10YR5/4) and dark yellowish brown (10YR4/2). Its resistant, ledgy beds dip 40° to S45°E, and are the uppermost Yeso strata exposed (Fig. 3.38).

Overlying beds of the Glorieta Sandstone have the same strike and dip and are about 30 m thick. These sandstones are fine-grained, supermature quartz arenites that display abundant trough crossbeds. Unmetamorphosed Glorieta beds are moderate orange pink (5YR8/4) to light brown (5YR6/4) and weather dark yellowish brown (10YR4/2). Beds that have been metamorphosed to metaquartzites are darker, grayish hues.

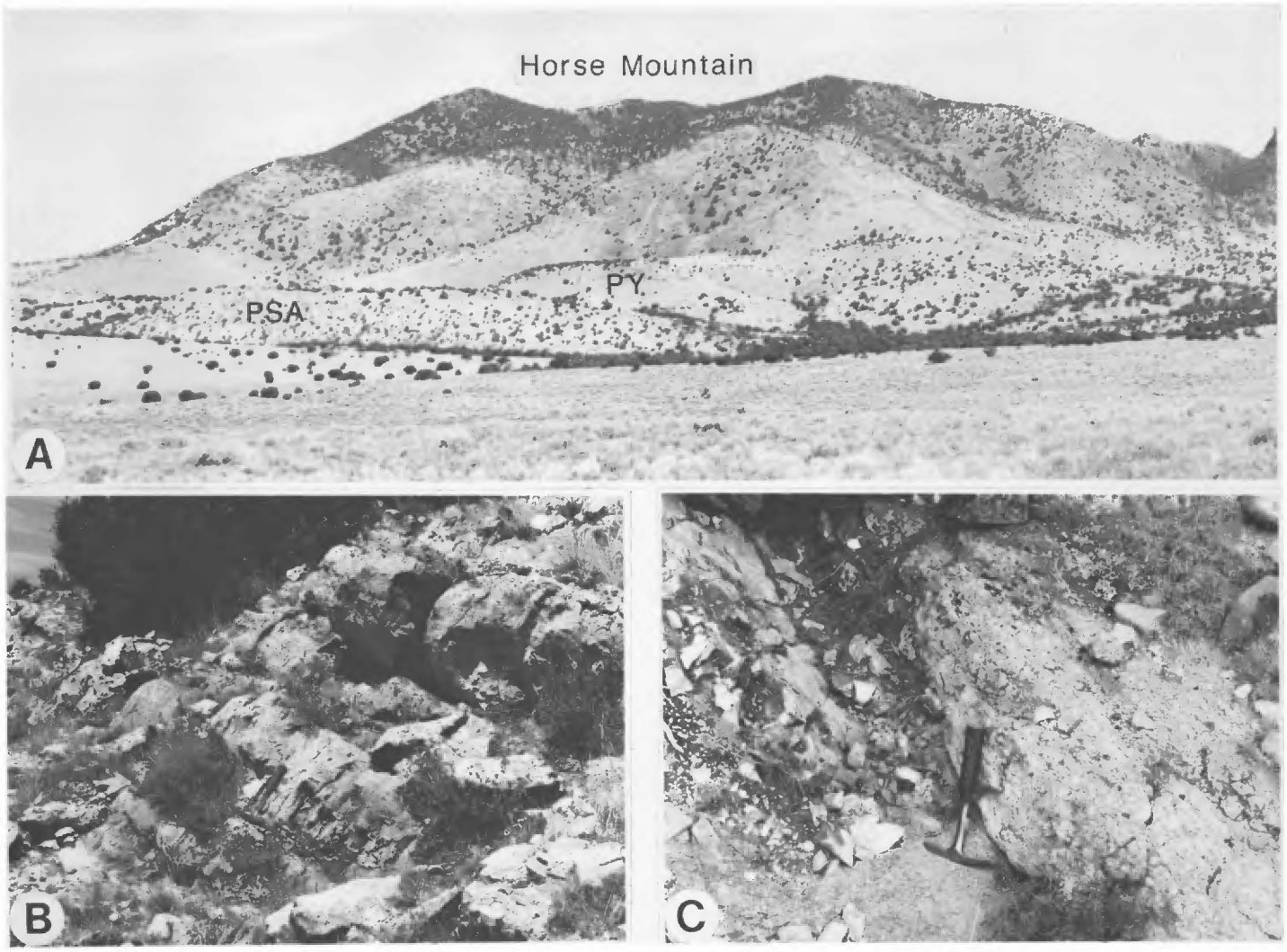

FIGURE 3.39. Permian strata south of Horse Mountain. A, Overview of Horse Mountain, looking north-northwest with San Andres Formation (PSA) hogback in foreground, underlain by Glorieta (not seen) and Yeso (PY) strata. B, San Andres limestones and dolomites on the hogback crest. C, Fault breccia (to right of hammer) in streamcut on north end of San Andres hogback dipslope.

The great majority of Permian strata south of Horse Mountain belong to the San Andres Formation, which is 115 m thick here. Most San Andres units are light brownish gray (5YR6/1) and pinkish gray (5YR8/1) micrites and dolomites (Figs. 3.38, 3.39B). Some limestone strata, especially those at the crest of the hogback, contain dark gray chert nodules. The San Andres fossils described below were collected from the crest of the hogback in a 3-m-thick bioclastic limestone interval about 83 m above the base of the formation.

At the base of the north dip slope of the hogback is a distinctive fault that tops the section. In the streamcut to the southwest, the hogback strata dip 30° to N20°W and are a mixture of grayish orange pink (10R8/2) to pale red (5R6/2) beds of fine-grained, gypsiferous, mature quartz sandstone and fault breccia consisting of limestone and sandstone clasts cemented by euhedral calcite crystals and gypsum veinlets (Hayden and Lucas, 1989). These sandstones belong to the Yeso Formation (Lucas and Hayden, 1989; O. Anderson, oral commun., 1993), and do not resemble Triassic sandstone to the north.

The Horse Mountain Permian strata show many similarities to Permian units 80 km to the north, in the Zuni Mountains of Cibola County. Indeed, the Horse Mountain outcrops can be added to the fence line for Permian strata extending from the Zuni Mountains to north of Pie Town (Colpitts, 1989, fig. 3). Yeso strata exposed at Horse Mountain are dolomites and sandstones referable to the Torres Member. The overlying Joyita Member of the Yeso present in the Zuni Mountains has pinched out to the south between about Pie Town and Horse Mountain. The Glorieta Sandstone is continuous across this area, although relatively thin at Horse Mountain. The tripartite division of the San Andres Formation—lower calcareous dolomite, middle cross-bedded sandstone, and upper dolomitic limestone—can no longer be discriminated at Horse Mountain (Fig. 3.40).

The San Andres Formation at Horse Mountain is locally fossiliferous, but preservation of specimens is poor. Most bivalves are represented by steinkerns and molds, and the shells of other groups are coarsely recrystallized or adhere closely to the hard limestone matrix, making extraction of intact, nonexfoliated specimens for study nearly impossible. These factors precluded precise identification of most taxa. The fauna is strongly dominated by molluscs, mainly bivalves and gastropods, with smaller numbers of nautiloids and the scaphopod *Prodentalium canna* (White). Moderate numbers of brachiopods (unidentified small productoids and *Composita*) and sparse echinoid and trilobite fragments are also present.

Bivalve taxa include at least nine species. Small to medium-size steinkerns of *Schizodus* are common; the shape and proportions of some specimens suggest *S. supaiensis* Winters, but others are higher and subtrigonal, closer in shape to *S. altus* Newell and Boyd. None of the specimens can be referred to *S. canalis* Branson, a common constituent of San Andres faunas to the northwest, near St. Johns, Arizona (Newell and Boyd, 1975) and Ojo Caliente, New Mexico (Kues and Lucas, 1989). *Leptodesma* (*Leptodesma*) aff. *sulcata* (Geinitz), *Promytilus retusus* Chronic, and *Sanguinolites*? sp. (of Chronic, 1952 and Winters, 1963) are each represented by one to a few specimens. Steinkerns of several small, laterally compressed, elongate species with anterior beaks are fairly abundant, but lacking preservation of hinge structures and shell ornamentation, they cannot be identified. These probably belong to *Permophorus*, *Edmondia* and possibly *Prothyris*. A small subtrigonal nuculanid, probably *Phestia perumbonata* (White) (see Yancey, 1978) displays the fine concentric step-rib ornamentation that characterizes this group.

Several species of low- and high-spired gastropods are present in this fauna, but available specimens are too severely weathered for identification. Specimens of *Bellerophon* (*Bellerophon*) sp. are moderately common, as are relatively large specimens (up to 40 mm wide) of *Straparollus* (*Euomphalus*) *kaibabensis* Chronic. This species is distinguished by large, well-spaced, rounded nodes along the dorsolateral margin of the whorls.

Insofar as can be determined from these rather sparse and poorly preserved remains, this fauna suggests a Leonardian age, consistent with that of the San Andres Formation in central New Mexico. The scaphopod *Prodentalium canna* is common in Lower Permian strata across the western U.S., and other molluscs from the Horse Mountain locality, such as *S.* (*E.*) *kaibabensis*, are conspecific with or closely related to species described from the Kaibab (Chronic, 1952) and/or upper Supai (Winters, 1963) formations of eastern Arizona, both of which are of Leonardian age.

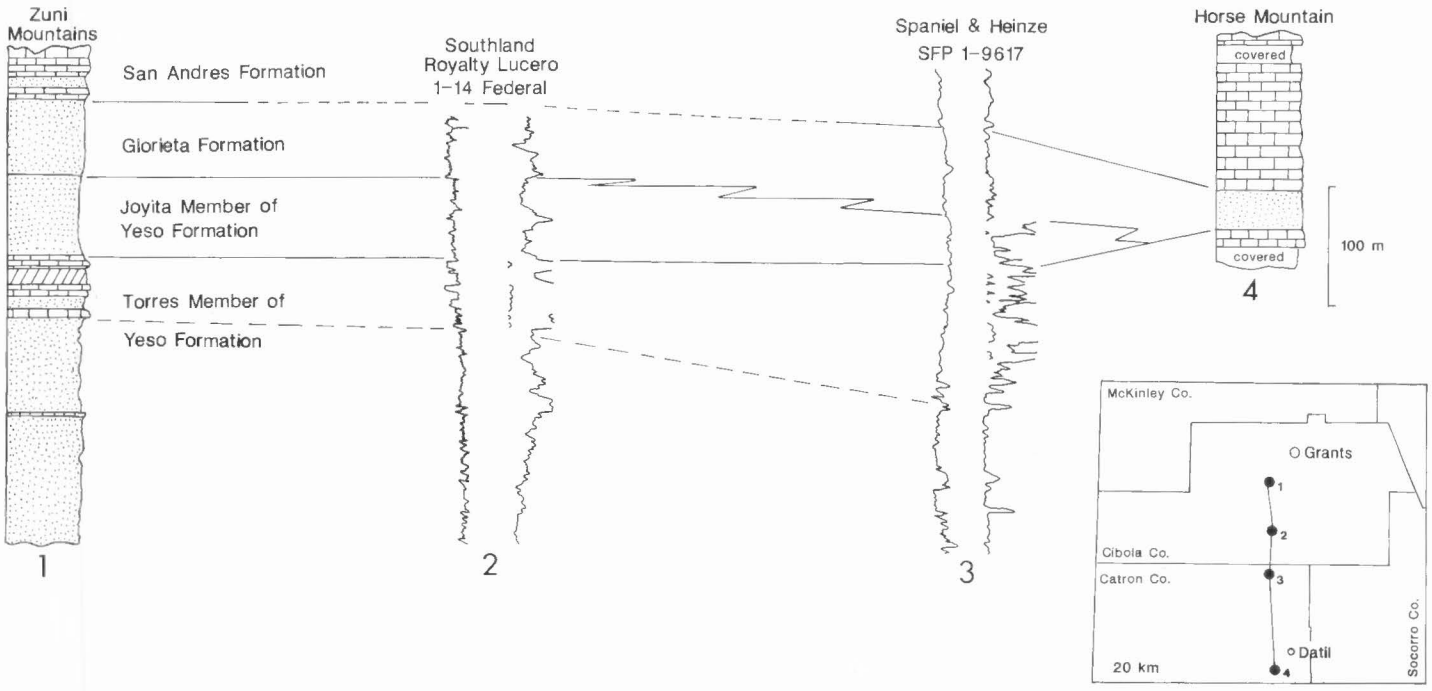

FIGURE 3.40. Correlation of Permian strata between the Zuni Mountains and Horse Mountain, west-central New Mexico (modified from Colpitts, 1989).

110.3 MP 54. Deep canyon north of highway slices into the central part of the Horse Mountain volcano, where a dacitic plug is surrounded by vent breccia and lava flows. Incomplete detailed geologic mapping in the Horse Mountain East quadrangle (Ratté, unpubl. 1991), old and new isotopic ages, and paleomagnetic analysis indicate that younger eruptive rocks may fill a crater surrounded by an older flow sequence in the crater walls. **2.0**

112.3 MP 56. Small isolated butte north of highway (Fig. 3-41) consists of Horse Mountain lava flows that are the same as those in the northeast ridge of Horse Mountain. This small hogback might be interpreted as a landslide block, but because there seems to be no obvious place from which it has slid, it is interpreted here as down-dropped on a buried northeast-trending fault along the mountain front. Conventional K-Ar and fission track ages of rocks related to the Horse Mountain volcano all indicate mid-Miocene eruption. For the central plug, we have a K-Ar plagioclase age of 12.0 ± 3.0 Ma, a zircon fission-track age of 10.4 ± 1.3 Ma, and a spurious K-Ar hornblende age of 35.3 ± 6.1 Ma. From the east ridge flow, we have K-Ar ages of 14.4 ± 0.6 Ma (plagioclase), and 13.7 ± 0.5 Ma (biotite), and a new Ar/Ar hornblende age of 12.64 ± 0.06 from the flow at the downdropped butte. These ages are all roughly consistent with the fission-track age from the central intrusion of 13.7 ± 2.1 Ma, reported earlier by Jones (1980). Another K-Ar age for biotite in tuff breccia, poorly exposed in a ravine beneath the east ridge flow, is 13.4 ± 1.1 Ma. The tuff breccia may be part of the initial cone of the volcano. A distinctive trachyte flow that has large (0.4-1.2 in.) sanidine phenocrysts crops out along the mountain front southwest of the east ridge flow (Fig. 3.41); it has a conventional K-Ar sanidine age of 11.2 ± 0.6 Ma. Beneath it is a basalt flow with a preliminary Ar/Ar age of 13.55 Ma. In addition, a mafic dike on the north side of the east ridge has a K-Ar whole rock age of 17.5 ± 2.1 Ma. Most ages cited here are from Marvin et al. (1987), and unpublished ages from Harold Mehnert (personal commun., 1991); the two new Ar/Ar ages are by Bill McIntosh. Additional Ar/Ar dating and paleomagnetic analysis are currently in progress for support of a more complete interpretation of the evolution of this volcano, and its regional volcano-tectonic relationships. **1.0**

113.3 MP 57. Good outcrops north of highway, on the nose of the east ridge of Horse Mountain, expose upper Datil Group ash-flow tuffs beneath the east ridge flow of the Horse Mountain volcano. Tuffs include the Datil Well Tuff and the tuff of Farr Ranch(?), separated only by a cooling break, and Rock House Canyon Tuff and Blue Canyon Tuff. Northeast of Horse Mountain, and separated from it by a northwest-trending buried fault, the low hills capped by Datil Well Tuff and tuff of Farr Ranch are largely buried by fanglomerate. **1.0**

114.3 MP 58. Luera Mountain, across the plains east of highway at 2:00-3:00 (Fig. 3.42), is a Bearwallow Mountain Andesite shield volcano at the northeast end of the line of andesitic volcanos that parallels the southeast edge of the Plains of San Agustin. This andesitic volcano has a central plug(?) of rhyolitic composition on the east side of Luera Peak, that has given a whole rock conventional K-Ar age of 25 Ma (Harold Mehnert, oral commun., 1988). Pelona Mountain and O Bar O Mountain are other andesitic shield volcanoes in this alignment along the south side of the plains that are visible from here at about 4:00 and 5:00, respectively. Both volcanoes have central plugs of medium-grained andesite and are about 25-26 Ma (Marvin et al., 1987). **2.0**

116.3 MP 60 is about 0.1 mi beyond the north edge of Horse Mountain East quadrangle. Highway cuts across southeast corner of Log Canyon quadrangle and into Sugarloaf Peak quadrangle about 1.85 mi ahead in the Quemado 1:100,000 quadrangle. Sugarloaf Mountain, north of highway, is at the southern end of the Crosby Mountains (Fig. 3.43), which consist mainly of volcaniclastic sedimentary rocks of the Oligocene South Crosby Peak Formation and tuffs and lava flows of the Mogollon Group. **5.0**

121.3 MP 65. Low, rounded outcrops and quarry on right are quartz diorite intrusion of Cerrito Viejo (Fig. 3.44), for which we have a conventional K-Ar biotite age of 30.2 ± 1.1 Ma, and a zircon fission- track age of 21.4 ± 2.3 Ma (Marvin et al., 1987), which are supported by a new Ar/Ar plagioclase age of 30.6 ± 1.4 Ma (McIntosh and Chamberlin, this guidebook). However, most of the roadcuts between here and Datil, about 9 mi ahead, are in the older Hells Mesa Tuff (32 Ma), which was previously mapped as the tuffs of Rock Tank and Ary Ranch (Lopez and Bornhorst, 1979), at the top of the Datil Group.

The South Crosby Peak Formation has been suggested as the fill of the proposed Crosby Mountains cauldron (Elston, 1984; Bornhorst, 1976; Jones, 1980), and the distribution of the South Crosby Peak Formation is within the outline of the proposed cauldron on the State Highway Geologic Map (NMGS, 1982). Other structural elements cited as part of the Crosby Mountains cauldron by Elston, Bornhorst and Jones consist of a proposed peripheral graben and a resurgent dome centered just southwest of Horse Mountain.

As discussed at Stop 3, we suggest that a caldera related to eruption of the Blue Canyon Tuff and the Horse Springs dacite may be buried beneath the Plains of San Agustin, but the eruption of the Horse Springs dacite as the principal cause of collapse for such a caldera seems unlikely because of its apparent small volume. The proposal that the South Crosby Peak Formation fills such a caldera seems to be untenable because the South Crosby Peak Formation is approximately 3.9 Ma younger (McIntosh and Chamberlin, this volume) than the proposed caldera-forming rocks (Blue Canyon Tuff and Horse Springs dacite). The suggested resurgent dome (Bornhorst, 1976, p. 81) is based on Stearns' description of "a broad, gentle dome underlying the lowlands southwest of Horse Mountain" (Stearns, 1962, p. 33). The area referred to is one of largely isolated outcrops of thin, upper Datil Group ignimbrites surrounded by alluvium (Ratté et. al., 1990). Most of the ignimbrites there are older than the Blue Canyon Tuff, and thus if they are part of a

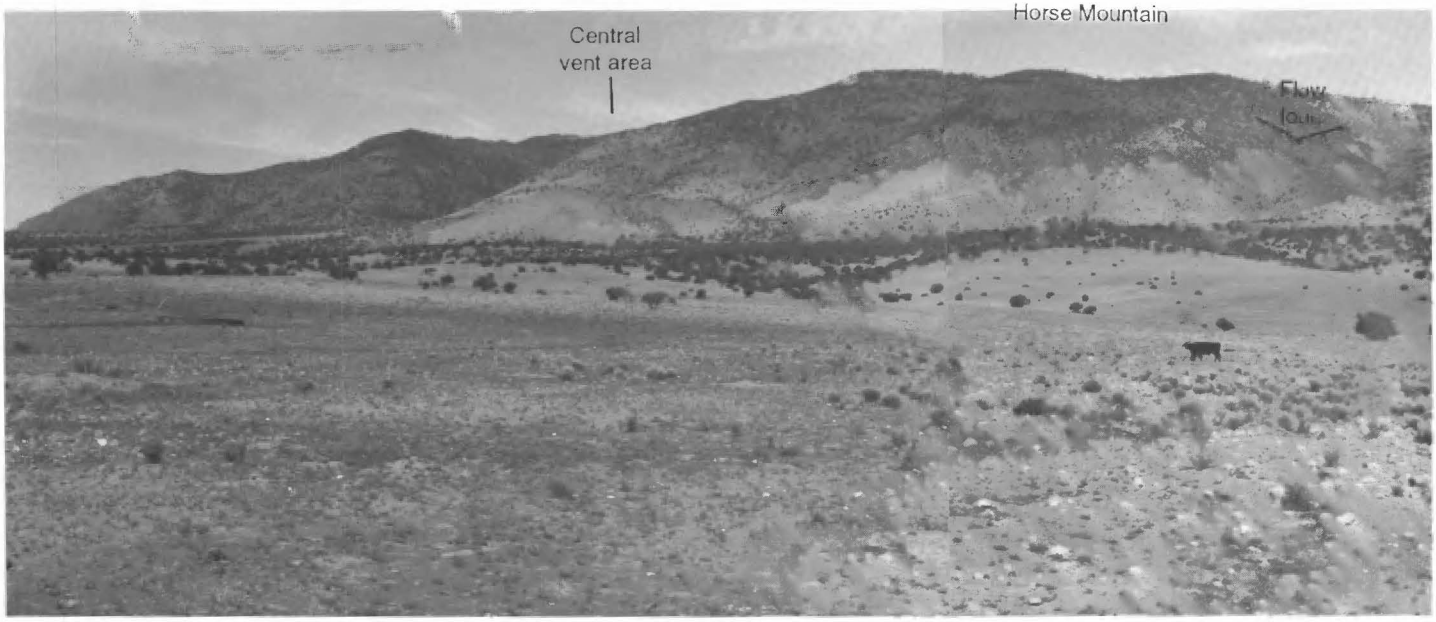

FIGURE 3.41. Panoramic view of Horse Mountain volcano from NM-12 at about MP-56.

resurgent dome, they must represent either the floor of the related caldera, or megabreccia from the caldera wall. The idea of a megabreccia from the *wall* (presumably northern wall) of a Blue Canyon Tuff caldera is appealing because some of the ignimbrite outcrops are broken into blocks that are separated by slickensided fractures. Thus a caldera, if present, and its resurgent dome, if any, would seem to have to be quite different from the geometry of the Crosby Mountains depression as proposed by Elston (1984). Chamberlin (see First Day road log) suggests that the "Crosby Mountains caldera" as defined by Elston (1989) represents a disparate collage of temporally unrelated structural elements. **3.0**

124.3 MP 68. Approaching roadcuts in Hells Mesa Tuff (32 Ma), which is the ledge-forming unit west of the highway. **1.0**

125.3 MP 69. Northern part of Crosby Mountains on left (northwest of highway); Anderson Mountain at about 10:00; East Sugarloaf Mountain at about 11 o'clock (Fig. 3.45). **2.5**

127.8 Roadcut in uppermost of three ash-flow tuffs interlayered with volcaniclastic rocks of South Crosby Peak Formation. Oldest of the three tuffs has an Ar/Ar plagioclase age of 29.7 ± 0.1 Ma. **1.0**

128.8 Road junction on left. Roadcut ahead on left is Hells Mesa Tuff. **1.9**

130.7 Road junction, NM-12 and US-60. Socorro, New Mexico is approximately 60 mi to the east on US-60. **End of road log.**

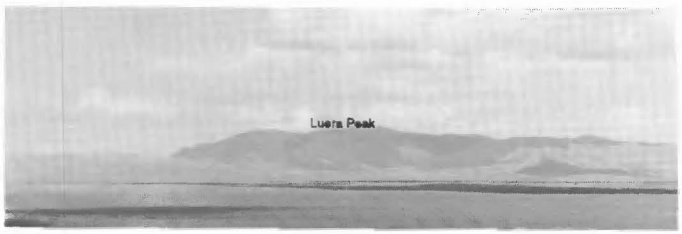

FIGURE 3.42. Luera Peak in the Luera Mountains, on the east side of the Plains of San Agustin east of NM-12 at about MP 58. Luera Peak marks the approximate eruptive center of the northeasternmost of the Bearwallow Mountain Andesite volcanoes that are along the southeast margin of the San Agustin graben.

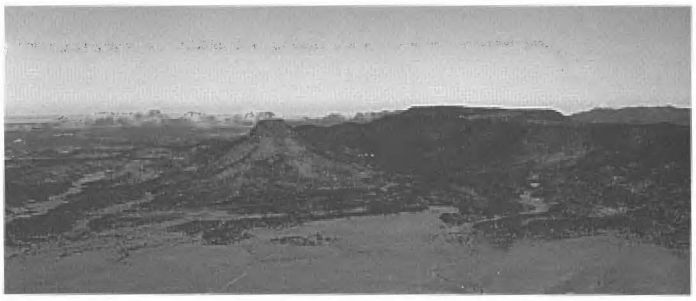

FIGURE 3.43. Aerial view, from south, of Sugarloaf Mountain at the southern end of the Crosby Mountains; Sawtooth Mountains in background left. Sugarloaf Mountain and mesa to right are underlain mainly by volcaniclasic rocks of South Crosby Peak (out of photo to right) and capped by basaltic andesite of Crosby Mountains and thin white Vicks Peak Tuff (28.5 Ma) beneath the capping flows.

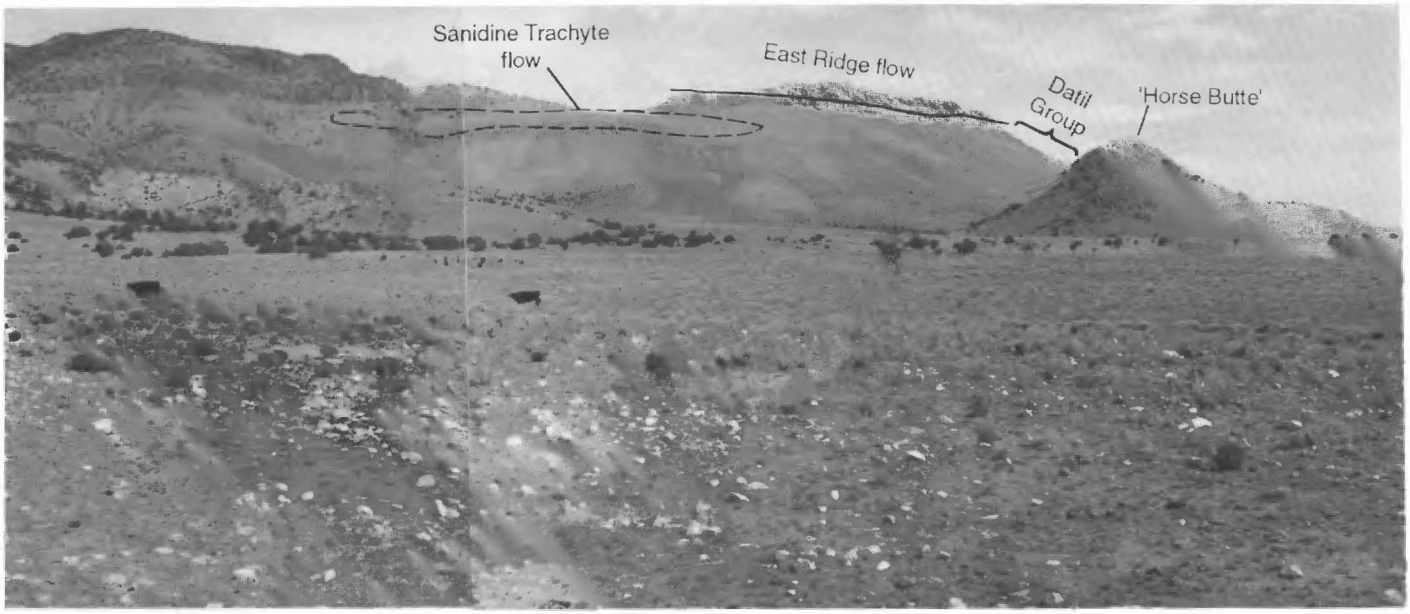

FIGURE 3.41. Panoramic view of Horse Mountain volcano from NM-12 at about MP-56.

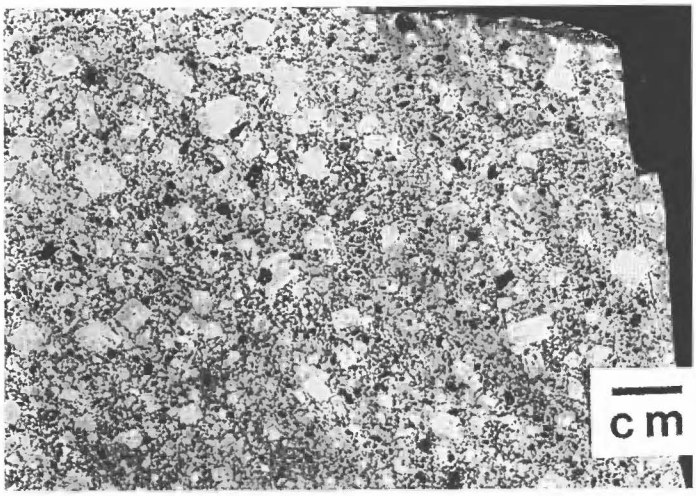

FIGURE 3.44. Slab of Cerrito Viejo intrusive rock showing seriate porphyritic texture consisting of fine- to coarse-grained phenocrysts of plagioclase, biotite and hornblende in a microcrystalline groundmass of equivalent composition. Sample NM-1114 of McIntosh and Chamberlin (this volume); collected from southeast side of road-metal quarry.

FIGURE 3.45. Aerial view of northern Crosby Mountains; Sawtooth Mountains in background center; Datil Mountains in background right. Crosby Mountains consist mainly of South Crosby Peak volcaniclastic rocks, capped by basaltic andesite of Crosby Mountains. Hells Mesa Tuff (32 Ma) crops out in low terrane on both sides of NM-12, from left to right across center of photo, and in highway cuts.

San Francisco Mountains and canyon of San Francisco River north of Reserve, New Mexico. View is N28°W. Gila Formation in foreground and middle ground is fill of Jon S half graben deposited against and faulted along the Saliz Mountains-Higgins Mountain fault of the Reserve graben system. In background, cliffs of the San Francisco River Box are formed mostly by andesite of Dry Leggett Canyon in the footwall of the San Francisco Mountains fault zone. Dillon Mountain, on skyline behind the box, is another upthrown block of mostly andesite of Dry Leggett Canyon. Camera station is alongside Highway 12 in SW ¼ sec. 36, T6S, R19W, approximately 3 km north of Reserve. Altitude is about 1825 m. Wayne Lambert photograph No. 93L66. August 14, 1993, 3:24 p.m. MDT.